A probabilistic rainfall model to estimate the leading-edge lifetime of wind turbine blade coating system

Verma, Amrit Shankar; Jiang, Zhiyu; Caboni, Marco; Verhoef, Hans; van der Mijle Meijer, Harald; Castro, Saullo G.P.; Teuwen, Julie J.E.

DOI
10.1016/j.renene.2021.06.122

Publication date
2021

Document Version
Final published version

Published in
Renewable Energy

Citation (APA)
Verma, A. S., Jiang, Z., Caboni, M., Verhoef, H., van der Mijle Meijer, H., Castro, S. G. P., & Teuwen, J. J. E. (2021). A probabilistic rainfall model to estimate the leading-edge lifetime of wind turbine blade coating system. *Renewable Energy*, *178*, 1435-1455. https://doi.org/10.1016/j.renene.2021.06.122

Renewable Energy 178 (2021) 1435–1455

Contents lists available at ScienceDirect

Renewable Energy

journal homepage: www.elsevier.com/locate/renene

A probabilistic rainfall model to estimate the leading-edge lifetime of wind turbine blade coating system

Amrit Shankar Verma [a, d, *], Zhiyu Jiang [b], Marco Caboni [c], Hans Verhoef [c], Harald van der Mijle Meijer [c], Saullo G.P. Castro [a], Julie J.E. Teuwen [a]

[a] Faculty of Aerospace Engineering, Delft University of Technology (TU Delft), Delft, 2629 HS, the Netherlands
[b] Department of Engineering Sciences, University of Agder, Grimstad, Norway
[c] TNO, Westerduinweg 3, 1755, LE Petten, the Netherlands
[d] SINTEF Ocean AS, Trondheim, Norway

ARTICLE INFO

Article history:
Received 27 June 2020
Received in revised form
31 May 2021
Accepted 26 June 2021
Available online 5 July 2021

Keywords:
Wind turbine blade
Leading-edge erosion
Probabilistic analysis
Analytical method
Long term analysis

ABSTRACT

Rain-induced leading-edge erosion of wind turbine blades is associated with high repair and maintenance costs. For efficient operation and maintenance, erosion models are required that provide estimates of blade coating lifetime at a real scale. In this study, a statistical rainfall model is established that describes probabilistic distributions of rain parameters that are critical for site-specific leading-edge erosion assessment. A new droplet size distribution (DSD) is determined based on two years' onshore rainfall data of an inland site in the Netherlands and the obtained DSD is compared with those from the literature. Joint probability distribution functions of rain intensities and droplet sizes are also established for this site as well as for a coastal site in the Netherlands. Then, the application of the proposed model is presented for a 5 MW wind turbine, where the model is combined with wind statistics along with an analytical surface fatigue model that describes lab-scale coating degradation. The expected lifetime of the blade coating is found three to four times less for the wind turbine operating at the coastal site than for the inland site - primarily due to rainfall at higher wind speeds. Further, the robustness of the proposed model is found consistent with varying data periods used for the analyses.

1. Introduction

1.1. Background

The continuous demand in the growth of renewable sources of power production has led to rapid growth in the wind energy sector. Wind turbines, both at onshore and offshore locations, are in high demand and it is expected that by 2050, half of the EU's1 electricity demand will be met by wind energy alone [1]. In order to achieve this goal, the current market trend involves deploying turbines with higher power ratings, along with turbines deployed at locations with larger wind speeds [2] such as near coastal and offshore locations. Such classes of turbines are profitable to the industry [3], however, this also presents enough challenges to the wind turbine owners and operators [4], especially from a maintenance perspective. For instance, large size blades rotating at high tip speeds are exposed to harsh environmental conditions such as frequent exposure to rainfall (Fig. 1(a)), thereby causing material degradation at the blade's leading-edge [5] - commonly referred to as rain-induced leading-edge erosion (LEE) of WTBs (Fig. 1(b)). The impact between rain droplets and the rotating blade at high tip speeds, typically in the range of 70–110 m/s [6,7], develops large impact pressure, subsequently leading to a combination of complex damage modes such as pitting, roughening of the leading-edge surface, fatigue failure of the blade coating, and eventually structural damage [8]. In Ref. [9], it has been found that LEE increases the drag coefficient of the aerofoil section by more than 314% and decreases the lift coefficient by around 53%, thereby reducing the overall aerodynamic efficiency of the WTB. The damage modes associated with LEE and their effects on the turbine's performance can appear in less than two years of the blade's service life, while

* Corresponding author. Faculty of Aerospace Engineering, Delft University of Technology (TU Delft), Delft, 2629 HS, the Netherlands.
E-mail addresses: a.s.verma@tudelft.nl (A.S. Verma), zhiyu.jiang@uia.no (Z. Jiang), marco.caboni@tno.nl (M. Caboni), hans.verhoef@tno.nl (H. Verhoef), harald.vandermijlemeijer@tno.nl (H. van der Mijle Meijer), s.g.p.castro@tudelft.nl (S.G.P. Castro), J.J.E.Teuwen@tudelft.nl (J.J.E. Teuwen).

https://doi.org/10.1016/j.renene.2021.06.122

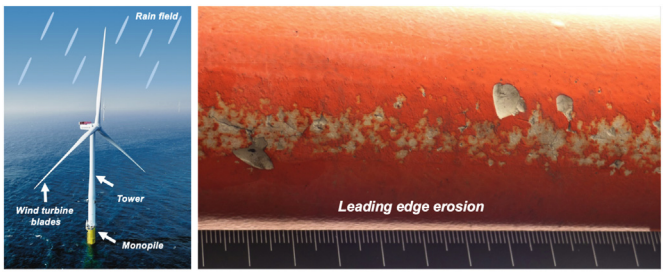

Fig. 1. (a) Wind turbine exposed to rain field [Source: Vattenfall group [12]](b) Examples of rain-induced LEE [Source: TNO [13]].

the blade is expected to last for atleast 15 years continuously. As a result, costly repair and maintenance work is imperative to be performed in order to maintain the design power curve of the wind turbine, thereby contributing to the overall increase in the cost of energy. It has been reported in Refs. [10,11] that LEE repair and maintenance expenses cost the European offshore wind turbine sector over £56 million annually, and hence LEE of WTBs requires urgent attention.

In view of this problem, it is essential to develop tools and methods that can aid the blade manufacturers and designers to choose the best coating solutions for WTBs. One of the important parameters is the expected lifetime of the blade coating system, which will provide real scale performance of the chosen blade coating solution for different sites and aid the turbine operators in planning maintenance and repairs expected over a lifetime. As per wind farm owner reports, some turbines require repairs as frequent as two years while others may run for many years without repairs [10,14]. Therefore, tools and methods that can provide site specific estimates about the expected life of coatings are essential.

Several research efforts are currently being undertaken to develop methods to obtain a reliable estimate of the expected lifetime of the blade coating systems. For instance, advanced leading-edge coating materials are tested under accelerated rain erosion tests using Whirling Arm Rain Erosion Rig (WARER) [15,16], jet erosion test facilities [17,18] as well as Single Point Impact Fatigue Tester (SPIFT) [19]. However, due to reasons such as lack of correlation between the accelerated rain test facility and realistic rainfall scenarios, experimental investigations are limited in representing the real scale coating performance and only provide comparative analysis of one coating against the other [20]. One of the main important limitations is that in the lab setting, only a limited number of representative test cases and rainfall conditions are simulated and the analysis process is deterministic. However, a rainfall event exhibits a stochastic nature, consisting of random parameters such as rainfall intensity and droplet size, and these parameters have varying probabilities of occurrence for different sites. Hence, it becomes absolutely essential to include site-specific stochastic treatment of rain and wind parameters for calculating a realistic lifetime of the blade coating systems during blade rotation.

In addition, high fidelity computational LEE models have also been developed to study the leading-edge erosion of wind turbine blades. These models range from coupled fluid structure interaction (FSI) methods [5,19,21–24] to decoupled Computational Fluid Dynamics (CFD) - Finite element Method (FEM) [25]. These studies mostly focus on single rain droplet response onto the coating specimen, with an aim to understand the erosion process. However, these numerical models are computationally extensive, and require several input material properties for using a reliable damage criterion. Also, it is a demanding task to extend the structural analysis results obtained from a single droplet impact to many random rain drops to estimate a realistic expected lifetime of the coating. Such an attempt has been carried out in Refs. [26–28] where computational frameworks were presented to link the impact stresses obtained from a random rain field to the expected lifetime of the blade coating system. For instance, a new stress interpolation method was developed in Ref. [27] to calculate impact stresses of all rain drops in a random rain event using which fatigue analysis was performed for a given site. Nevertheless, these methods did not consider the site specific characteristics for a wind turbine site and the probabilistic treatment of associated rain and wind parameters were not taken into account for calculating the expected lifetime of the blade coating system.

Unlike the above discussed numerical models that are computationally demanding and lack site-specific stochastic treatment of rain and wind parameters, analytical based LEE models are more commonly used by the industry to estimate leading-edge (LE) lifetime of the coating system. This is due to the fact that these models are (1) simple, (2) systematic (3) require limited number of input parameters, (4) can link together various interdisciplinary models (rain, structural, wind turbine etc.) as well as (5) aid in robust correlation of results obtained in the lab and in-situ observations. On top of that, aerospace industries [29] have a wide experience with such models as they have been applied widely in the past to mitigate erosion and cavitation problems related to steam turbine blades [30], airfan blades [31] as well as optical transmission losses in aircraft and spacecraft windows [32]. In the current study, the main emphasis is placed on improving such analytical based LEE models by including a site-specific probabilistic treatment of rain and wind parameters to obtain a reliable estimate of the lifetime of a LE coating system. A brief description about the framework for a typical analytical LEE model as well as some of the important terms that are specific to the paper are introduced and discussed below. Furthermore, the scope and novelty of the current work will be defined.

1.2. Analytical LEE models

There exist a wide variety of analytical-based LEE models in the literature such as - Springer's model for homogeneous materials [33], Springer's model for coated specimens [34], Springer's model for fiber reinforced composites [35], Siemens' LEE model [36], TNO's fatigue model [17], and DTU's kinetic energy model [37] to name a few. Fig. 2 presents a general architecture for a typical LEE model, which requires four distinct input parameters: (a) *Rainfall statistical model* that includes defining the statistical characteristics of the rain data for a wind turbine site, consisting of parameters such as rainfall intensity (I) and droplet diameter (φ_d), recorded using rain gauges and disdrometers, (b) *Wind turbine model* that gives information such as the type, class, location as well as the associated power curve of the wind turbine together with wind statistics of the site, (c) *Impingement model* that describes the number of rain droplets that will actually hit the rotating WTB during precipitation and (d) *Material model* consisting of fatigue properties of the coatings. All the above input parameters are combined through different expressions and finally fed to LEE models. These models yield the following output parameters as shown in Fig. 2: (a) incubation period i.e. the time until which there is no significant mass loss in the coating which implies negligible aerodynamic losses of the wind turbine, (b) linear rate of mass loss, i.e. the rate at which the coating loses the mass upon exposure to rain implying a need for repair and maintenance, and finally (c) the total time to coating failure which implies a significant loss in power output. The incubation period defined in Fig. 2 is regarded in this paper as 'expected leading-edge lifetime of the blade coating system' and refers to the duration of insitu time that will require no erosion induced repair activities.

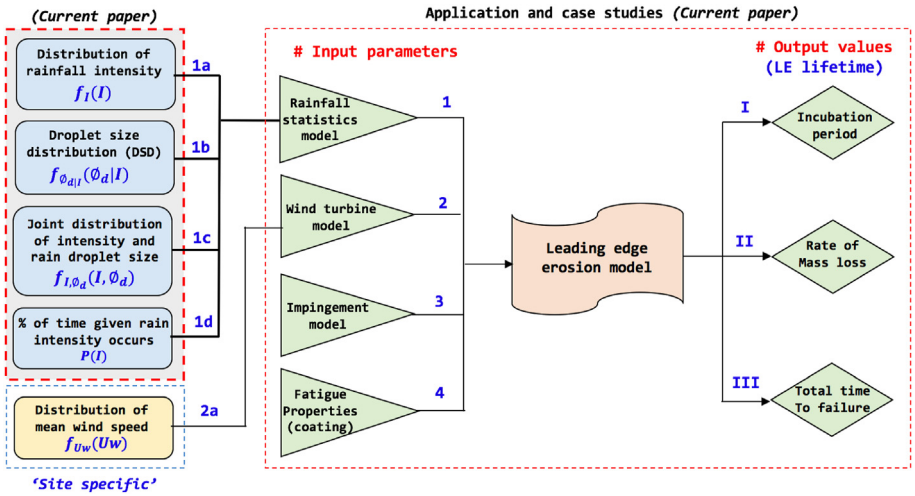

Fig. 2. General architecture and inputs required for leading-edge erosion models.

As described above, one of the essential input parameters for LEE models includes defining the site-specific statistical characteristics of the rainfall such as rainfall intensity and the rain droplet size. In the literature there have been very few attempts to include these aspects in the LEE models. For instance, current industry standard feed the droplet sizes in the LEE model based on published DSDs, such as Best's distribution [38] and Marshall-Palmer distribution [39]. This involves choosing a representative droplet size (such as median droplet diameter, D_{50}) for different ranges of rain intensities. One of the disadvantages of this approach is that during the analysis, only the droplet size is considered as a probabilistic statistical parameter, which do not reflect site sensitivity and lack stochastic treatment. Additionally, both rainfall intensities together with droplet diameters are statistically dependent random variables which are stochastic in nature and must be defined through a joint probabilistic distribution. Further in the model, it is also important to include the effects of dry periods for a given site when there is no rain recorded, given that blade rotation on these days will not contribute towards the rain-induced LEE. Recently, the effects of dry periods as well as statistical dependence between rainfall intensity and the rain droplet size have been included in Ref. [14]. The rain parameters from the raw rainfall data were directly fed to the kinetic energy based LEE model from Ref. [37] to calculate the expected lifetime of the coating system and it was hypothesized that the erosion occurs during a few extreme precipitation events. However, the work presented did not give any considerations about how sensitive the estimated values are to the data periods used for the analysis and the approach lacked a pure probabilistic framework.

In the present paper, it is hypothesized that the probabilistic distribution of the rainfall parameters, referred to as probabilistic rainfall model, is a more consistent input form for the LEE model to determine the expected LE lifetime, and the erosion is a result of consistent exposure to rainfall rather than a few extreme precipitation events. The probabilistic rainfall model proposed in the paper describes the measured precipitation data for a given site through three different probabilistic distributions (refer to the three blue colored blocks in Fig. 2): (a) marginal distribution of rainfall intensity ($f_I(I)$), (b) the conditional distribution of rain droplet size given the rainfall intensity ($f_{\varphi_d|I}(\varphi_d|I)$), also referred to as droplet size distribution (DSD), and (c) joint probability distribution of rainfall intensity and rain droplet size ($f_{I,\varphi_d}(I,\varphi_d)$), that describes the statistical dependence between rain intensity and rain droplet size. Further, the effects of dry period are quantified by the fourth block in the rainfall model (Fig. 2) which is the measure of percentage duration of time when different rain intensities actually occur at the site ($P(I)$). However, it is assumed in the paper that rain and wind parameters are statistically independent, and wind statistic is described through the marginal distribution of wind speed at the hub height (refer to the yellow colored block in Fig. 2 which is connected to the wind turbine model). This distribution will determine the expected tip speed with which blade will rotate during the service life while interacting with the rain - thereby contributing to the overall accumulated damage over the lifetime. More details are discussed in the subsequent sections.

1.3. Novelty and scope of the current paper

To the authors' knowledge, no existing work describes a probabilistic model using which statistical rain parameters of a given site can be fed to an LEE model to determine the site-specific expected life of the blade coating. Hence, one of the main novelties of this paper is to establish a probabilistic rain model, determine different distributions of the statistic rain model for different sites in the Netherlands and demonstrate their application by evaluating the expected lifetime of the blade coating system through case studies.

The scope of the current paper is divided into two main parts: (a) *the first part* is focused on establishing a probabilistic rainfall model itself. A series of steps will be considered such as determining a new droplet size distribution (DSD) based on two years of onshore rainfall data measured by KNMI using the Thies Clima disdrometer at the inland De Bilt site in the Netherlands. Further, the proposed DSD is compared with the most frequently used DSD from the literature i.e. Best's DSD [38] and recently published DSD [40]. Next, the marginal distribution of the rainfall intensity together with mean wind speed at hub height is established for the above stated inland site as well as for the coastal De Kooy site in the Netherlands, and joint probability distribution functions of rain intensity and droplet size are established. (b) *The second part* of the paper deals with the application of the proposed probabilistic rainfall model through case studies where expected life of a wind turbine blade coating is calculated for inland and coastal sites by considering NREL 5 MW wind turbine.

The remainder of the paper proceeds as: Section 2 presents the literature review on different probabilistic distributions of the rainfall model. Section 3 defines the analysis procedure. Section 4 describes the site and dataset description as well as the

methodology involved. Section 5 discusses the details of the case study. Section 6 presents and discusses the results. Section 7 concludes the paper. Finally, section 8 provides limitation and recommendations for future work.

2. Literature review related to probabilistic distributions of rainfall model

In this section, a brief summary is made on some of the past work carried out in the literature on different distributions that make up the probabilistic model proposed in the paper.

2.1. Marginal distribution of rainfall intensity ($f_I(I)$)

A rainfall event is described by (a) the amount of rain defined by the rainfall intensity (I) as well as (b) occurrence of rain that include both data points - some positive numbers (that describe the occurrence of rainfall i.e, wet periods) and 'zero rainfall' (no occurrence of rain i.e. dry period) [41]. Generally, positive records of dataset are used for determining the distribution for rainfall intensity, whereas the occurrence of rain is dealt as a separate process. Here, the literature review is presented dealing with distribution fits for non-zero rainfall dataset. The aspect of occurrence of rainfall is considered in the paper through $P(I)$ i.e. by quantifying the percentage duration of time when different rain intensities occur at the site.

One of the first work on this aspect was presented by Kedem et al. [42] for modelling the rainfall intensity where different distributions including lognormal and gamma were used. The rain data from weather station at Darwin and Florida in the USA were utilised. It was found that the lognormal distribution fit the data more accurately than the gamma distribution as well as other parametric distributions defined in the paper. Cho et al. [43] compared the gamma and lognormal distribution for describing rain rates measured using Tropical Rainfall Measuring Mission (TRMM) satellite, and minimum χ^2 method was utilised to estimate their distribution parameters. The results show that the Probability Density Function (PDF) of both the distributions described the rain data satisfactorily. However, it was found that the gamma distribution underestimates the light and heavy rainfall intensity, whereas lognormal distribution underestimates the intermediate rainfall intensity.

It is to be noted that most of the work in the literature considers comparison of lognormal and gamma distribution for fitting rainfall intensity for a site, given that these distributions are skewed to the right, which is generally is seen as a characteristic feature of rainfall intensity data.

Nevertheless, there is no common consensus regarding which distribution is the best, and in the literature other distributions are also utilised. Salisu et al. [44] compared the Generalized Pareto, exponential, beta and gamma distribution to judge the best fit for marginal distribution of rainfall intensity ($f_I(I)$) representing hourly rain data at twelve stations at peninsular Malaysia. Different goodness of fit testing methods such as - Kolmogorov-Smirnov (KS) test, χ-square test and Anderson-Darling tests were explored, and it was found that all the distributions can be used to describe the rain intensity at the site. Nevertheless, Generalized Pareto distribution outperformed all the other four probabilistic distributions used. Adiku et al. [45] utilised rain data at two sites in Ghana, and twenty years of rainfall data, along with Markov model and two parameter distributions. The results in the study clearly show that the rainfall data is well represented by gamma distribution. In summary, there is plenty of work describing the best distribution fit for rainfall intensity for a given site, and thus the available knowledge can be applied to the proposed model.

2.2. DSD, or conditional distribution of rain droplet size given the rainfall intensity ($f_{\varphi_d|I}(\varphi_d|I)$)

Rainfall intensity alone as a statistical parameter is not sufficient to describe a rain event. Individual rain droplets impacting the blade during precipitation while the blade is rotating govern the accumulated fatigue damage of blade coatings, and influence the LEE of WTBs [36]. Consequently, it is essential to determine the rain DSD which describe the distribution of droplet size and their distribution in space. In general, the droplet size depends on multiple factors [38] that include - (a) rainfall intensity, (b) rain type (thunderstorm, orographic), (c) as well as relative humidity to name a few. However, in this paper, the focus is placed explicitly on DSD dependence on rainfall intensity alone. The first ever DSD that has been presented dates back to 1946, where an exponential distribution was proposed by Marshall and Palmer [39], also commonly known as Marshall-Palmer function, which is given by:

$$n(\varphi_d, I) = n_0 \cdot exp(-\lambda \varphi_d) \tag{1}$$

where, $n(\varphi_d, I)$ is defined as the number of droplets of diameter φ_d per unit volume of rainfall for a given rainfall intensity I, n_o is a constant that defines the $y-$intercept and is considered as $8 \cdot 10^3\ m^{-3}/mm$, and λ is the parameter of the exponential distribution, which is defined as the slope of $n(\varphi_d, I)$-φ_d curve on a semi-logarithmic plot. It was found that λ decreases with increasing I and is defined by the following power law (Eqn 2):

$$\lambda = 4.1 \cdot I^{-0.21} \tag{2}$$

where I is expressed in mm/hr. Marshall-Palmer fitted these data to observations from Ref. [46], and the results were found to be in good agreement (Fig. 3(a)). Some important observations through their study were - (a) As the rain droplet size increases, the number of droplets in a unit volume of rain reduces for any given I (b) median droplet size increases (D_{50}) with increasing rainfall intensity (c) both the number of smaller and larger rain droplets increases with increasing I, however, the increase in the number of droplets is significantly higher for larger droplet size. It is to be noted that the exponential model from Marshall-Palmer function gives a higher prediction for smaller droplets [47], with the number of droplets increasing monotonically for droplet size limiting to zero (Fig. 3(b)) and the distribution is inappropriately skewed to the lower end of the distribution. This is not a typical characteristic of a pragmatic rainfall, and therefore, several researchers in the past have tried to improve this model, such as the gamma distribution from Ref. [48] as well as the lognormal model from Ref. [49].

The above stated DSD and the associated analysis represent the rain droplets reaching the ground and are mostly applied to the problems related to soil erosion and flood issues in the catchment areas [38]. The problem related to LEE of WTBs require the DSD in the air, given that turbines are placed at large heights from the ground. Consequently, one of the most widely used DSD for LEE models is Best's distribution where the author presented a DSD in the air by dividing the number of drops of a given size reaching the ground by the associated terminal velocities [38]. There are other advantages of Best's distribution such as - *(a)* unlike Marshall-Palmer DSD, which gives number of droplets of a given size in a liquid rain and is inappropriately skewed to the lower end of the distribution, Best's DSD mostly focuses on estimating the volume of water droplets of a given size in the rain [36]. This makes Best's DSD insensitive to the size of rain drops, and *(b)* parameters of Best's DSD are obtained by averaging the rain data over several measurement sites that include Marshal and Palmar data, Canadian data, Ynysylas data, and Lenard rain data to name a few. Following

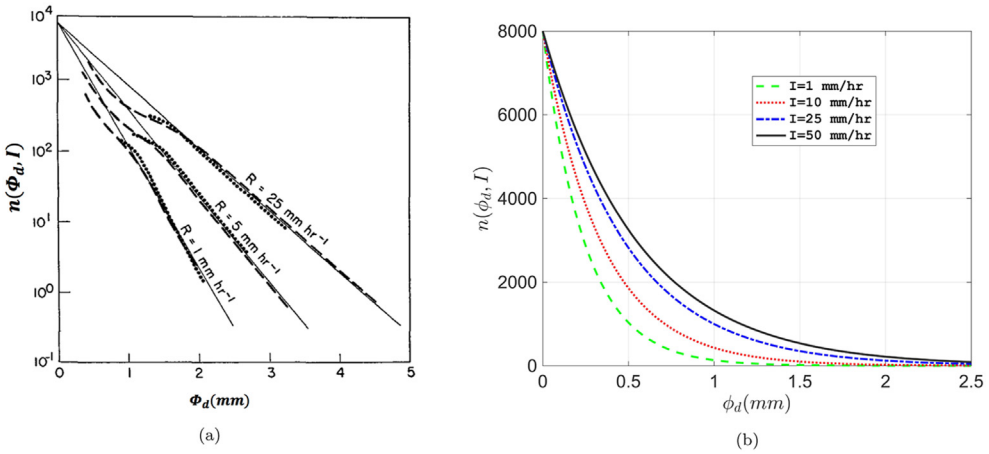

Fig. 3. (a) Comparison of the measured data with exponential function [39] (b) Typical characteridtic of Marshall-Palmer DSD for various *I*.

the analysis, the author in Ref. [38] gave a generalized DSD which is found to follow a two parameter Weibull distribution model defined as (Eqn 3):

$$F_{\varphi_d|I}(\varphi_d|I) = 1 - exp\left[-\left(\frac{\varphi_d}{a}\right)^n\right] \quad (3)$$

where, $F_{\varphi_d|I}(\varphi_d|I)$ is defined as the fraction of rain droplets with size less than or equal to φ_d for a given rainfall intensity (I) also considered as DSD in this paper, φ_d is the droplet diameter expressed in *mm*. a and n in the above equation are the scale and shape parameters of the Weibull distribution respectively that are related to I by the following relationship (Eqn 4 and 5):

$$a = A \cdot I^p \quad (4)$$

$$n = N \cdot I^q \quad (5)$$

where A, p, N and q are the constants in the above equation. In his paper, Best found that the shape parameter n is independent of I and the established constants are presented in Table 1. Overall, the general form of Best's DSD is (Eqn 6):

$$F_{\varphi_d|I}(\varphi_d|I) = 1 - exp\left[-\left(\frac{\varphi_d}{1.3 \cdot I^{0.232}}\right)^{2.25}\right] \quad (6)$$

Fig. 4(a) presents Best's DSD for different rainfall intensities (I), where it can be seen that as I increases, median droplet size (D_{50}) also increases as was observed before for Marshall Palmer function. Also, the distribution provides information about the volume (mass) of rain drops of a particular size present in a rain for a given I. For instance, as I increases, the fraction of volume contributed from large droplets is higher compared to smaller rain droplets.

Following the above stated benefits of Best's DSD, recently, a DSD was calculated for offshore conditions in the North Sea [40] using disdrometer data. Here, similar methodology as presented by Best was considered and the offshore DSD, also referred to as Catapult's DSD in the paper, was found to be described satisfactorily by two-parameter Weibull distribution. A comparison of their datasets with Best's DSD was presented, and it was concluded that Best's DSD was not suitable for offshore rain condition. However, the datasets for comparison represent only one year of disdrometer data of offshore and for only one site in the North Sea, compared to Best's DSD which is a generalized DSD calculated from multiple rain datasets. Also, unlike Best's DSD, the shape parameter n was found dependent on I (see eq. (7)), and the constants of the distributions were obtained and are presented in Table 1. Overall, the general form of Catapult's offshore DSD is given by (Eqn 7):

$$F_{\varphi_d|I}(\varphi_d|I) = 1 - exp\left[-\left(\frac{\varphi_d}{1.03 \cdot I^{0.138}}\right)^{2.83 \cdot I^{-0.0953}}\right] \quad (7)$$

Fig. 4(b) presents Catapult's DSD for different rainfall intensities I, where the median droplet size (D_{50}) increases with increasing I as expected. However, the stretch of the DSD is less for larger intensities compared to the Best's DSD. In the current paper, a new DSD will be developed based on the same methodology followed by Best [38] and Catapult [40] and constants of the eq. (4) and (5) will be determined for rainfall data measured by KNMI [50] using the Thies Clima disdrometer at the De Bilt site in the Netherlands. Further, the proposed DSD will be compared with the above-discussed DSDs. The methodology that is used to obtain these constants (A, p, N and q) will be presented in the next section.

Table 1
Constants determined for Best's and offshore Catapult's DSD.

DSD	Constants				
		A	*p*	*N*	*q*
	Best's DSD	1.3	0.232	2.25	0
	Catapult's DSD	1.026	0.1376	2.8264	−0.0953

2.3. Joint probability distribution of rainfall intensity and rain droplet size ($f_{I,\varphi_d}(I, \varphi_d)$)

Rainfall intensity together with droplet diameter are statistically dependent random variables and must be defined through a joint probabilistic distribution for a given site. The joint probability distribution of two random variables X and Y determines the probability of both the variables simultaneously occurring together. In general, for two dependent random variables X and Y, the joint distribution function ($f_{X,Y}(x, y)$) is defined by the following equations:

$$f_{X,Y}(x,y) = f_X(x) * f_{Y|X}(y|x) \quad (8)$$

where $f_X(x)$ is the marginal distribution of X, and $f_{Y|X}(y|x)$ is the conditional distribution of Y given X. Based on the above definition, the joint probability distribution function of rain droplet size and rain intensity can be defined as the product of marginal distribution of rain intensity and DSD and given by:

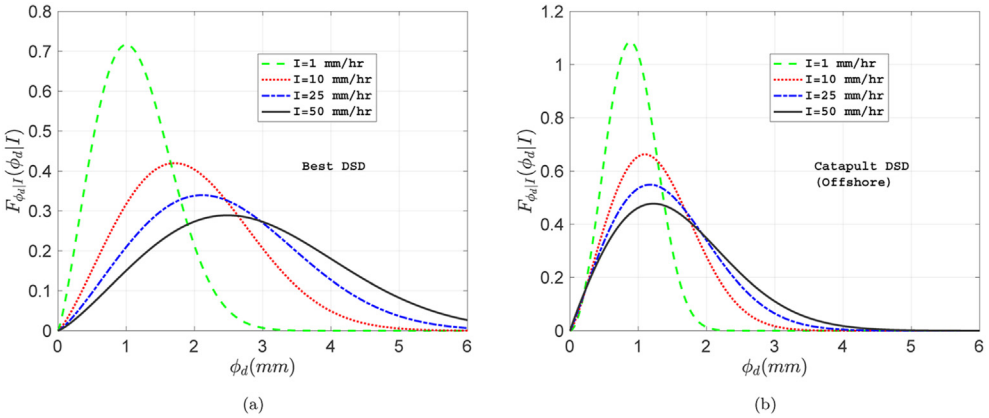

Fig. 4. Typical characteristics of (a) Best's DSD (b) Catapult's DSD for several *I*.

$$f_{I,\varphi_d}(I,\varphi_d) = f_I(I)\ ^{*} f_{\varphi_d|I}(\varphi_d|I) \tag{9}$$

Such a probabilistic approach is rare in the field of LEE of WTBs, however it has been widely utilised for long term fatigue analysis and reliability assessment in the OWT sector for monopile under different stochastic wind and wave loads. A similar approach has been recently utilised by Refs. [51,52] to calculate structural safety assessment and estimate average failure probability for blade installation task. Joint distribution function of random variables such as significant wave height H_s, wave spectral peak period T_p, and mean wind speed (U_w) is established and distribution parameters for different offshore sites in Europe have been presented [53].

3. Analysis procedure

Fig. 5 presents the flow chart describing the analysis procedure used in the paper for development and application of the probabilistic rainfall model. The flow chart also describes how different input models (shown in different background colours) - i.e. rainfall statistic model, wind turbine model, and material model are coupled together and fed to an analytical surface fatigue model to estimate the expected lifetime of the blade coating systems. Principally, the overall analysis procedure consists of seven distinct steps, where first four steps are related explicitly to the development of the probabilistic rainfall model which is the main focus of the paper (marked as steps *I*, *II*, *III*, and *IV* in the flow chart). The remaining steps are related to the other inputs required for the application part (steps *V* and *VI* are related to wind turbine model whereas step *VII* is related to material model which describes the material degradation of the coating). In the next section, the first part dealing with the development of the probabilistic rainfall model is presented. Further, in the next section, case study of the proposed model with description of the considered turbine type, coating properties and LEE model are presented.

4. Methodology: probabilistic rainfall model

4.1. Descriptions of the considered sites and rain datasets

The analysis is performed on rainfall data for two different sites - one corresponds to the inland De Bilt site and the other corresponds to the coastal De Kooy site (see Fig. 6). For the De Bilt site, there are two different rainfall datasets available: **(a)** rainfall dataset having record of droplet diameter (φ_d) and corresponding rainfall intensities (I) measured by Thies Clima disdrometer for a period of 2 years (February 2016–February 2018) **(b)** rainfall dataset having record of only the rainfall intensity data (I) measured by rain gauge and precipitation sensor for the past 50 years (1971–2020). On the other hand, for the coastal De Kooy site, only the latter rain dataset (b) is available. It is important to note that varying rainfall datasets are used for different purposes in the paper - disdrometer data are used to establish the droplet size distribution for the site, whereas the rain gauge data are used for determining the distribution of the rainfall intensity for the site. In addition, since the disdrometer dataset are not available for the coastal De Kooy site, Catapult's offshore DSD will be used for this site in the paper.

4.2. Droplet size distribution (DSD)-$f_{\varphi_d|I}(\varphi_d|I)$

In this section, the methodology for establishing the droplet size distribution (DSD) for the De Bilt site is discussed. The primary step is to determine the constants of the eqs. (4) and (5) described in section 2 i.e. *A*, *p*, *N* and *q*. An in-house script is prepared for the purpose of data processing where the first step includes sorting and identifying unique counts of different rainfall intensity (I) in the rainfall dataset. This is followed by counting the number of times these unique I are being repeated in the array. Different droplet sizes corresponding to each unique I are then grouped together, and each group is then plotted on a two-parameter Weibull probability paper to check if the droplet size data for a given I fits the distribution. The Weibull probability plot is given by the equation:

$$ln(-ln(1-F)) = n \cdot ln(\varphi_d) - n \cdot ln\ a \tag{10}$$

From the analysis, an array of scale (a) and shape parameters (n) are obtained for different I by using the above equation that takes the form of a straight line. Finally, the dataset of scale (a) and shape parameters (n) are plotted on respective scatter plots against rainfall intensity (I) having logarithmic axes, which are based on the following equations:

$$ln\ a = p \cdot lnI + ln\ A \tag{11}$$

$$ln\ n = q \cdot lnI + ln\ N \tag{12}$$

The line of best fit to the above scatter plots gives the constants *A*, *p*, *N* and *q* and represents the DSD for the entire rainfall dataset. Similar analysis is also performed for deriving these constants for different seasons in Netherlands to estimate the seasonal DSD - *Winter* (01 January to 31 March), *Spring* (01 April to 30 June), *Summer* (01 July to 30 September), and *Autumn* (01 Oct to 31 December).

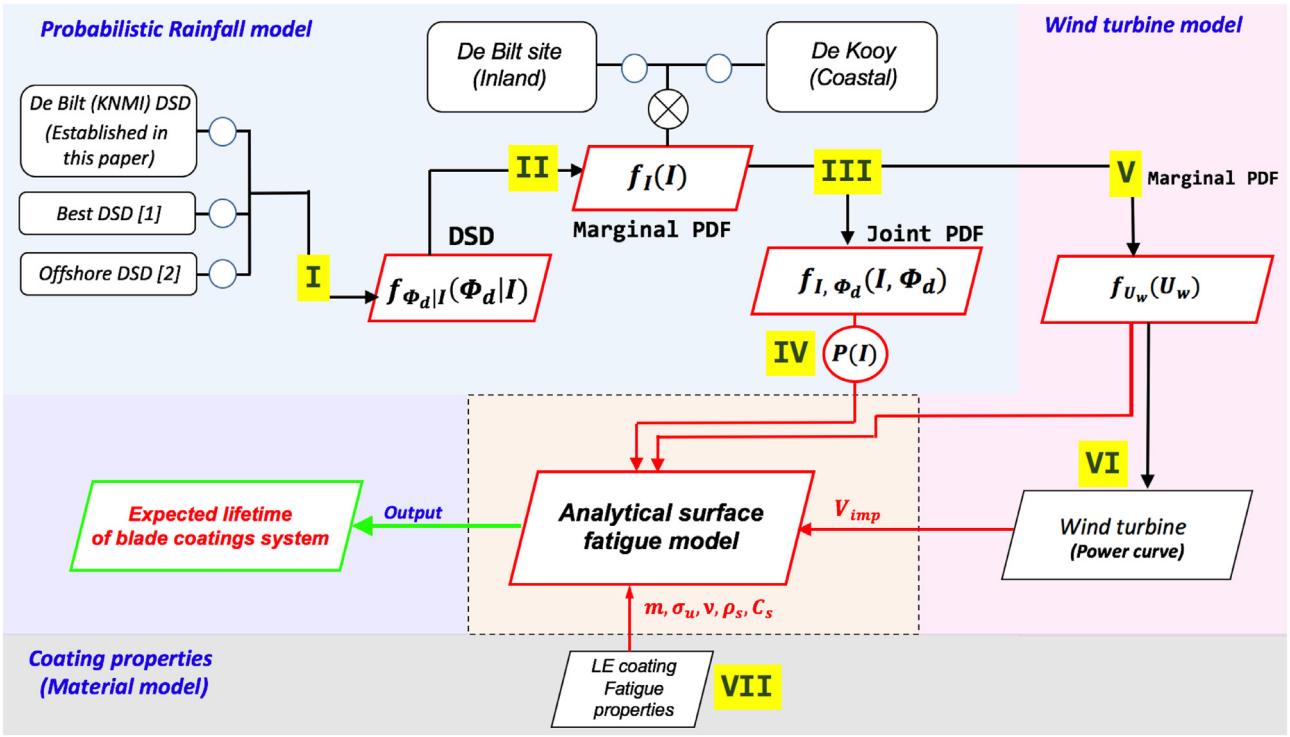

Fig. 5. Analysis procedure considered in the paper.

Fig. 6. Details of the site considered for the analysis [Modified from Ref. [54]].

4.3. Marginal distribution of rainfall intensity $f_I(I)$

For determining the most suitable distribution fit for describing the marginal distribution of rainfall intensity $f_I(I)$, two different distributions are compared - lognormal distribution and gamma distribution. The lognormal distribution is given by:

$$f(x) = \frac{1}{\sqrt{2\pi}\sigma_x} e^{-(\ln(x)-\mu_x)^2/2\sigma_x^2} \; ; \; x>0, \text{ and } \sigma_x>0 \tag{13}$$

where μ_x and σ_x are parameters of the distribution and are defined as mean and standard deviation respectively. On the other hand, gamma distribution is given by:

$$f(x) = \frac{x^{\alpha-1}e^{-x/\beta}}{\beta^{\alpha}\Gamma(\alpha)} \; ; \; x>0, \text{ and } \alpha>0, \; \beta>0 \tag{14}$$

where α and β are shape and scale parameters respectively. $\Gamma(\alpha)$ is defined as the gamma function which is given by the integral:

$$\Gamma(\alpha) = \int_0^{\infty} x^{\alpha-1}e^{-x}dx \tag{15}$$

For comparing these distributions, the rain data consisting of only the wet periods is plotted on their individual probability papers, as well as on their respective quantile-quantile plots ($Q-Q$ plot) to check which distribution best represents the rainfall intensity data. Further, the parameters for both the distributions are obtained by using Maximum Likelihood Estimation (MLE) method [55]. A χ^2 goodness of fit test is considered for both the distributions to perform hypothesis testing, where a significance level of 5% is considered for null hypothesis (H_o: Data is represented by the considered distribution). χ^2 goodness of fit test determines whether a dataset belongs to a specified probability distribution where the parameters are estimated from the data. In the χ^2 goodness of fit test, the entire dataset is grouped into several bins,

and then the observed and expected count is estimated based on which χ^2 value is determined given by the equation:

$$\chi^2 = \sum_{k=1}^{n} \frac{(O_k - E_k)^2}{E_k} \tag{16}$$

Once the χ^2 value is determined, this value is then compared with χ^2_{cric} value, which is obtained from a standard χ^2 distribution corresponding to a particular degree of freedom equal to $n-1-m$ and associated significance level α_s. Here n is the number of bins in which the entire dataset is divided, m is the number of parameters of the distribution used for the analysis which is taken as 2 for both gamma and log-normal distributions, and α_s is considered as 0.05 (5% significance level). It is then checked if the χ^2 value is less than χ^2_{cric}, and in that case, the null hypothesis (H_o: Data is represented by the considered distribution) cannot be rejected, and the distribution is found to represented by the considered distribution.

4.4. Joint probability distribution of rainfall intensity and rain droplet size ($f_{I,\varphi_d}(I,\varphi_d)$)

For the inland De Bilt site, the marginal distribution of the rainfall intensity is combined with the De Bilt's DSD. A comparison is also presented to show the joint distribution sensitivity to the choice of DSD by combining the marginal distribution of the rainfall intensity of the inland De Bilt's site with Best's DSD. On the other hand, for the coastal De Kooy site, the Catapult's offshore DSD [40] is combined with the marginal distribution of rain intensity given that the disdrometer dataset was not available for the DSD calculation.

4.5. Percentage of occurrence of rain of a given intensity (P(I))

The above discussed distribution parameters are determined by only including the wet periods for the considered site. However, it is equally essential to consider the dry periods for the considered sites when there was no occurrence of rain intensity, and based on that we can evaluate the total percentage of the occurrence of rain of a given intensity at a given site. In general, only these days will contribute towards the rain-induced LEE when the rain intensity is recorded. In order to calculate this, the whole rain dataset of 50 years consisting of both 'rain days' and 'no rain days' is considered, and percentage of occurrence of different range of intensities I in the rainfall dataset are calculated based on Table 2.

5. Application and case studies

One of the main applications of the proposed rainfall model is to estimate site-specific leading edge lifetime of blade coating system. In this section, the application of the proposed model is presented for a 5 MW wind turbine where the model is combined with wind statistics along with an analytical surface fatigue model that describes lab-scale coating degradation. The details are discussed in this section.

Table 2
Classification of different rainfall types [20].

Type of rainfall	Range of intensity
No rainfall	No I recorded
Light rainfall	$0 < I < 2.5$
Moderate rainfall	$2.5 \leq I < 10$
Heavy rainfall	$10 \leq I < 50$
Very heavy rainfall	$I \geq 50$

5.1. Wind turbine model

An open source NREL 5 MW wind turbine is considered for the analysis. The details of the wind turbine model are presented in the Table 3. The power curve of the wind turbine which determines the rotational speed of the blade under different operational mean wind speeds is presented in Fig. 7.

5.2. Wind statistic model

The rotational speed of the wind turbine blade is dependent upon the operational wind speed at the hub height. Therefore marginal distribution of mean wind speed at hub height is determined for both the inland and coastal sites considered in the paper. The data is available with reference to 10 m height and is extrapolated to 90 m hub height for the considered turbine using power law which is given by the equation:

$$U_w(z) = U_w(z_r) \cdot \left(\frac{z}{z_r}\right)^{\bar{\alpha}} \tag{17}$$

where $U_w(z)$ is the wind speed at any given height z, z_r is the reference height i.e. 10 m and $\bar{\alpha}$ is power law exponent considered as 0.14 for both the sites [57]. Two different distributions - Weibull and lognormal distribution - are compared through their respective $Q-Q$ *plot* and corresponding distribution parameters are obtained using Maximum Likelihood Estimation (MLE) method.

5.3. Description of LEE model, coating properties and long term assessment

The maximum impact velocity (V_{imp}) between raindrop and blade tip during the blade rotation can be approximately defined as:

$$V_{imp} = V_{blade} + V_{tg} \tag{18}$$

where V_{blade} is defined as the blade tip speed and depends upon the operational mean wind speed (U_w). V_{tg} is defined as the terminal velocity of the rain droplet and is dependent upon the rain droplet size (φ_d) defined in mm, V_{tg} (in m/s) is defined by the equation [58]:

$$V_{tg} = 9.65 - 10.3e^{-0.6\varphi_d} \tag{19}$$

The erosion damage rate calculated without considering the probability of occurrence of precipitation parameter for any given φ_d, I, and U_w is defined as the *short term erosion damage rate* ($\dot{D}_i^{ST}|I, \varphi_d, U_w$). The erosion damage rate (in hr^{-1}) is defined by the analytical surface fatigue model from Ref. [29]:

Table 3
Description of NREL 5 MW reference turbine [56].

Rating	5 MW turbine
Rotor orientation, configuration	Upwind, 3 Blades
Control Variable speed	Collective pitch
Rotor, Hub diameter	126 m, 3 m
Hub height	90 m
Cut-in, Rated, Cut-out wind speed	3 m/s, 11.4 m/s, 25 m/s
Cut-in, Rated rotor speed	6.9 rpm, 12.1 rpm
Rated tip speed	80 m/s

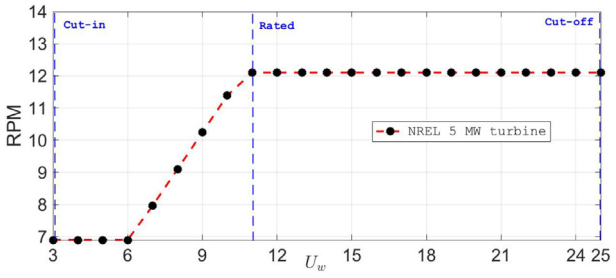

Fig. 7. NREL 5 MW turbine RPM v/s U_w curve.

$$\dot{D}_i^{ST}(I,\varphi_d,U_w)=\frac{\dot{N}}{N_{ic}}=\frac{\bar{q}\cdot V_{imp}\cdot\beta_d}{\frac{8.9}{\varphi_d^2}\left(\frac{S}{p_{wh}}\right)^{5.7}} \tag{20}$$

where $\bar{q}$ is the number of droplets per unit volume of rainfall which is given by:

$$\bar{q}=530.5\frac{I}{V_{tg}\varphi_d^3} \tag{21}$$

where I is defined in mm/hr. β_d is the impingement efficiency given by the relation:

$$\beta_d=1-e^{-15\varphi_d} \tag{22}$$

p_{wh} is the water hammer pressure defined by:

$$p_{wh}=\frac{\rho_w c_w V_{imp}}{1+\frac{\rho_w c_w}{\rho_s c_s}} \tag{23}$$

where ρ_s and c_s are density of coating and speed of sound in the coating material respectively. S is the erosive strength of coating material defined by:

$$S=\frac{4\sigma_u(m-1)}{1-2\nu} \tag{24}$$

where σ_u, m and ν are the ultimate tensile strength, Wohler's slope and Poisson's ratio of the coating material respectively.

Finally, an equation for *long-term erosion damage* rate is proposed in the paper which is given as the weighted sum of short term erosion damage rate together with probability of occurrence of all possible rain and wind conditions that are expected to occur during the blade's service life:

$$\dot{D}_i^{LT}=\sum_i^{\infty}\sum_j^{\infty}\sum_k^{\infty}\dot{D}_i^{ST}(I,\varphi_d,U_w)\cdot f_{I,\varphi_d}(I_i,\varphi_{dj})\cdot P(I_i)\cdot f_{U_w}(U_{w_k})\;\Delta I\;\Delta\varphi_d\;\Delta U_w \tag{25}$$

where $\dot{D}_i^{LT}\geq 1$ imply failure of coating material. The above method where short term responses are combined with long term distribution of all possible environmental condition is in general defined as the *long term probabilistic assessment* [59]. In the paper, different range of I, φ_d and U_w (I varies from $(0<I\leq 50$ mm/h), φ_d varies from $(0<\varphi_d\leq 6$ mm), and U_w varies from $(0<U_w\leq 30$ m/s) are considered such that eq. (26) is satisfied (total area under the PDF curves is approximately 1 to ensure contribution of damage from all possible environmental cases is taken into consideration for a given site):

$$\iiint_{i\,j\,k} f_{I,\varphi_d}(I_i,\varphi_{dj})\cdot f_{U_w}(U_{wk})\;dI\cdot d\varphi_d\cdot dU_w\approx 1 \tag{26}$$

Finally, the expected lifetime for the blade coating system, in years, is defined by ($\dot{D}_i^{LT}$ in hr^{-1}):

$$t_{years}=\frac{1}{\dot{D}_i^{LT}\cdot(365\cdot 24)} \tag{27}$$

In this study, a two component polyurethane based coating material is used to determine the erosion damage rate. The material properties are obtained by using an inverse method where the coating life observed in the WARER test is mapped with the estimates from the analytical Springer's model (Table 4). The WARER test results were obtained from the material datasheet [60] where the life of the coating before complete failure is described as more than 9 h for rain erosion test under 30–35 mm/h of rain, 2 mm droplet size and 123–157 m/s of impact velocity as per the ASTM G-73 [61] standard (see Table 4).

6. Results and discussion

In this section, results and discussion are presented. This section is also divided into two parts, where the first part (A) deals with the discussion of results related to the development of the probabilistic rainfall model whereas the second part (B) discusses the results related to the application of the proposed model where expected leading-edge lifetime of the coating system is calculated for both the considered sites.

6.1. Probabilistic rainfall model

6.1.1. Droplet size distribution (DSD)-$f_{\varphi_d|I}(\varphi_d|I)$

6.1.1.1. DSD: Determination of constants. Fig. 8(a)-(d) present the recorded rain droplet size (φ_d: droplet diameter) fitted to the two parameter Weibull probability papers for different unique counts of rainfall intensities ($I=0.5$ mm/h, 0.8 mm/h) as well as for different ranges of observed I (10 mm/h $<I<$ 20 mm/h; 20 mm/h $<I<$ 50 mm/h). The results clearly show that the two parameter Weibull distribution represents a sound representation of droplet size data given that the data points lie close to the black dotted straight line. Moreover, the coefficient of determination and least-standard error for these fits corresponding to all I are determined and Weibull distribution is found suitable for representing DSD for the site. The scale (a) and shape (n) parameters of the Weibull distribution are then obtained corresponding to each unique count of recorded I using MLE. In this way, an array of Weibull distribution parameters (a and n) are obtained. These parameters are then plotted on a scatter plot based on the eqs. (11) and (12) against rainfall intensity, with scatter plot defined with logarithmic axes (Fig. 9(a)-(b)).

Table 4
Material properties for polyurethane coating.

Parameter	Values	Units
ρ_s	1020	kg/m^3
c_s	2480	m/s
σ_u	37	MPa
m	6.1	–
ν	0.42	–

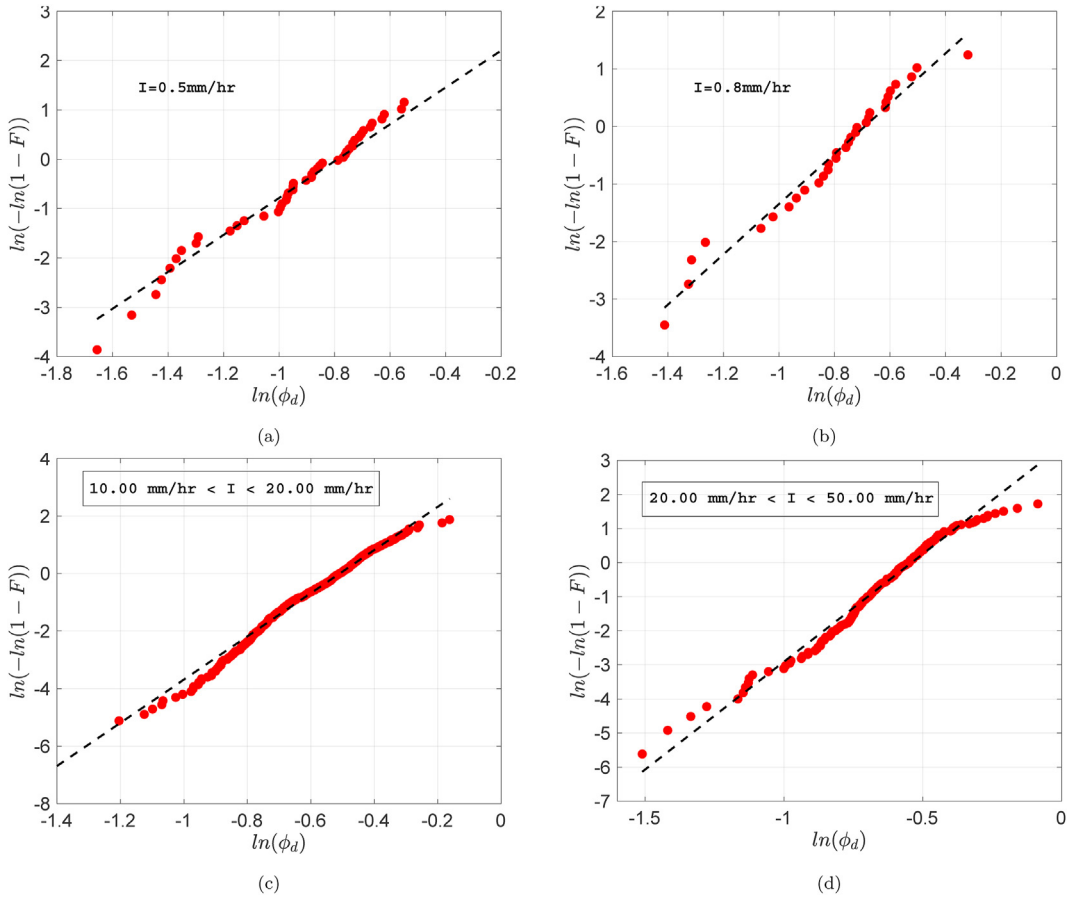

Fig. 8. Two-parameter Weibull fitting of rain droplet diameter (φ_d) for different (a) $I = 0.5$ mm/h (b) $I = 0.8$ mm/h (c) 10 mm/h < I < 20 mm/h (d) 20 mm/h < I < 50 mm/hr

Note that unlike Best's distribution, the shape parameter (n) is found to vary with the rainfall intensity (I), and is in line with the observation made by Ref. [40] for the droplet size measured by disdrometer for Catapult's offshore DSD. Finally, the line of best fit for both the scatter plots gives the constants of the DSD i.e. A, p, N and q and are tabulated in Table 5. Overall, the DSD corresponding to the De Bilt site recorded through the disdrometer has the form:

$$F_{\varphi_d|I}(\varphi_d|I) = 1 - exp\left[- \left(\frac{\varphi_d}{0.4811 \cdot I^{0.1186}} \right)^{4.56 \cdot I^{0.14}} \right] \quad (28)$$

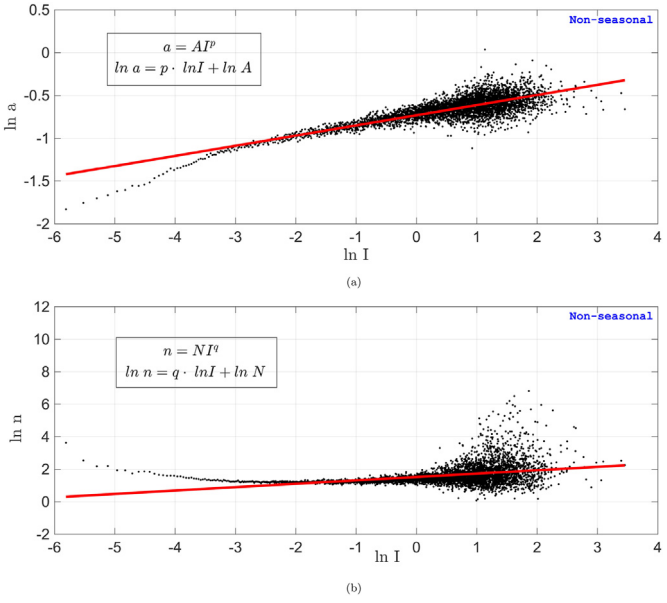

Fig. 9. (a) Calculation of constants A and p (b) Calculation of constants N and q using scatter plots.

6.1.1.2. Description of De Bilt's DSD and its comparison with existing DSDs. Fig. 10(a)-(b) present the probability distribution function (PDF) and cumulative distribution function (CDF) curve for the rain droplet size corresponding to the De Bilt's DSD, describing different rainfall intensities (I = 0.1 mm/h, 1 mm/h, 10 mm/h, 50 mm/h, 100 mm/h). The results from both the figures show that as I increases, median droplet size (D_{50}) also increases. Also, the distribution provides the information about the fraction of volume of rain drops of a particular size present in the rain for a given I. For instance, as I increases, the fraction of volume contributed from large droplets is higher compared to smaller rain droplets. These observations about the droplet size and volume of rain drops

Table 5
Constants determined for DSD at the De Bilt site.

A	p	N	q
0.4811	0.1186	4.567	0.1404

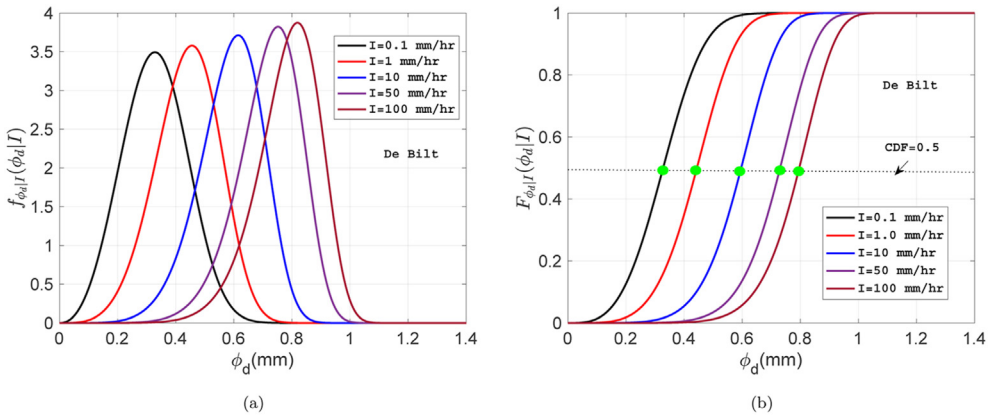

Fig. 10. Characteristics of De Bilt's DSD (a) PDF (b) CDF (I = 0.1 mm/h, 1 mm/h 10 mm/h, 50 mm/h, 100 mm/h).

contained in the rain are in line with the pragmatic characteristics of a typical rain DSD and verifies the accuracy of the obtained DSD.

Fig. 11(a)-(f) present the comparison between De Bilt's DSD determined in this paper with Best's DSD and Catapult's offshore DSD utilised in the literature for analysis of LEE of WTBs. The comparisons are made between the probability distribution function (PDF) and cumulative distribution function (CDF) curve for the rain droplet sizes corresponding to different I's (I = 0.1 mm/h, I = 1 mm/h, I = 10 mm/h). Some important observations are: (1) For very low rainfall intensity, the characteristics of all the three DSDs are in close agreement, however, the difference in the statistical representation of the droplet size by all these DSDs increases with increasing rainfall intensity, (2) There is a large deviation in the rain droplet size characteristics between onshore and offshore rainfall, and Best's DSD together with De Bilt's DSD does not represent a good fit for the offshore rain, (3) The data at De Bilt site cannot be represented by existing DSDs and the error will be significant especially for higher rain intensity, (4) The rain droplet size

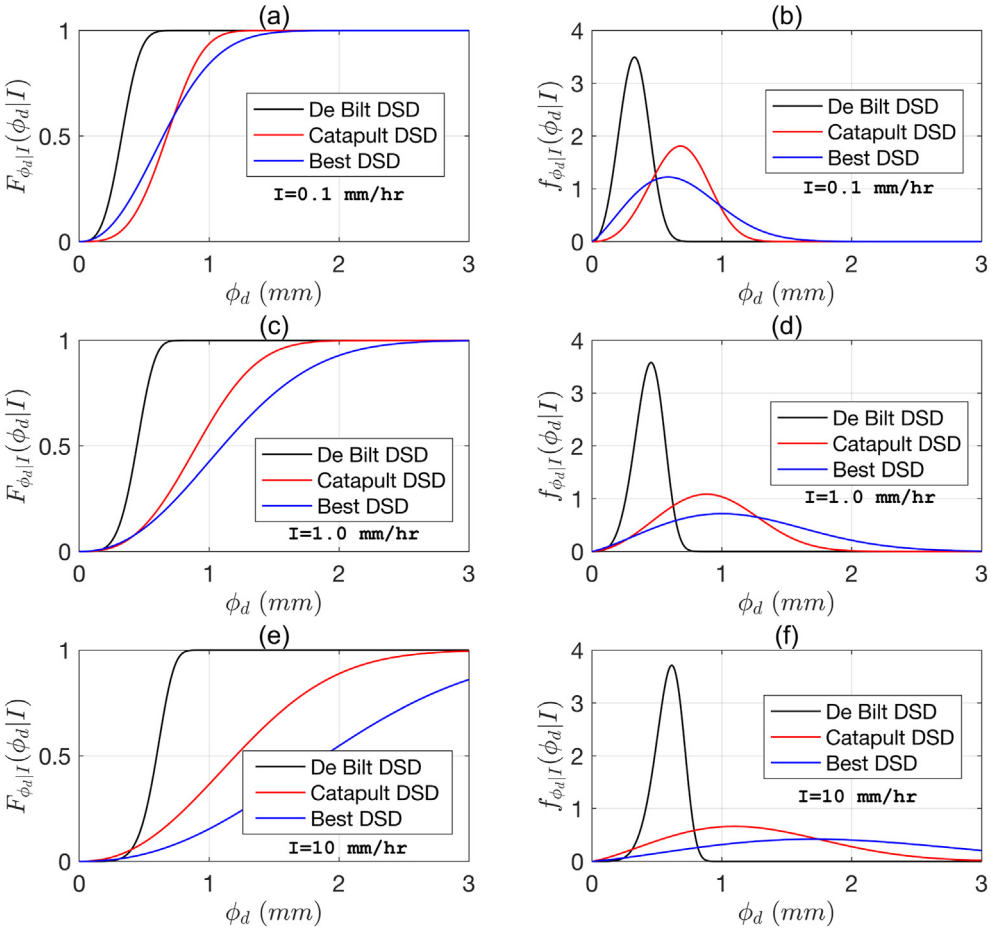

Fig. 11. Comparison of De Bilt's DSD with Best's DSD and Catapult's DSD (I = 0.1 mm/h, 1 mm/h 10 mm/h).

described by De Bilt's DSD are mostly capped below 1 mm, and is in line with the recorded raw rainfall data. Overall, DSDs are site specific distributions and must de defined independently for different wind turbine sites. This also implies need for installing more disdrometers in the future.

One of the analysis approaches for LEE of WTB in general includes selecting a representative rain intensity and corresponding median rain droplet size. For instance, in Ref. [5], $I = 2$ mm/h, $I = 10$ mm/h, $I = 25$ mm/h and $I = 50$ mm/h represented light, moderate, heavy and very heavy rainfall conditions respectively, and then based on a typical DSD, a droplet size corresponding to $CDF = 0.5$ is considered as the median (representative) droplet size. Fig. 12(a)-(c) present the CDF curve of rain droplet size representing rainfall described by Best's, Catapult's and De Bilt's DSDs respectively. The point where the black solid line intersects the CDF curve represents the median droplet size (D_{50}), and is represented by red dots for Best's DSD, blue dots for Catapult's offshore DSD, and green dots for De Bilt's DSD. As observed before, the median droplet size increases with increasing rainfall conditions for all the DSDs, however it is Best's DSD that seems to over predict the median droplet size for each rain intensity. This can also be seen from Fig. 11(d), where a quantitative comparison for median droplet size (D_{50}) is made for Best's, Catapult's and De Bilt's DSDs and for $I = 2$ mm/h, $I = 10$ mm/h, $I = 25$ mm/h and $I = 50$ mm/h. The representative droplet size for Best's distribution is 2.74 mm for $I = 50$ mm/h, whereas for the Catapult's DSD it is 1.48 mm, and for De Bilt's DSD the median droplet size is 0.73 mm. This implies that not all sites for LEE analysis can be described by Best's DSD, as there can be large deviations in the estimates of the representative sizes.

One of the important consequences of differences in the median droplet sizes (D_{50}) estimated by different DSDs is the effect on the number of droplets that occur in the rainfall for a given I. This is due to the fact that q is inversely proportional to cube of droplet size (see eq. (21)). As a result, though De Bilt's DSD and Catapult's DSD predict smaller droplets for a rainfall with the same intensity, there will be large number of drops in a unit volume of rainfall compared to Best's DSD that predicts larger droplet sizes. This is expected to influence the fatigue of the WTBs as there will be relatively more number of hits during the blade rotation. A quantitative comparison of the number of droplets per unit volume of rainfall is presented in Fig. 13 for De Bilt's, Catapult's and Best's DSD, for different values of I ($I = 2$ mm/h, $I = 10$ mm/h, $I = 25$ mm/h, $I = 50$ mm/h) and corresponding median droplet size (D_{50}) with the figure defined with the logarithmic y-axis. The results show that the number of drops are significantly larger for the same amount of rain for De Bilt's DSD compared to Best's DSD. The corresponding dots on the curve represent the median droplet size for a given rainfall intensity.

6.1.1.3. Determination of seasonal De Bilt's DSDs. The above discussed DSDs represent non-seasonal DSDs calculated for the rain data recorded by the disdrometer for the entire period of 2 years. Here, the DSDs are presented for seasonal variations of rainfall for the De Bilt site in Netherlands - *Winter*, *Spring*, *Summer*, and *Autumn*. The procedure used in the previous discussions for determining the non-seasonal DSDs is considered and the constants A, p, N and q are determined for each season. Fig. 14(a)-(d) present the scatter plot, where two parameter Weibull distribution parameters determined for different unique counts of I corresponding to different seasons are plotted on a scatter plot against rainfall intensity with logarithmic axes. The line of the best fit corresponding to each scatter plots gives seasonal parameters

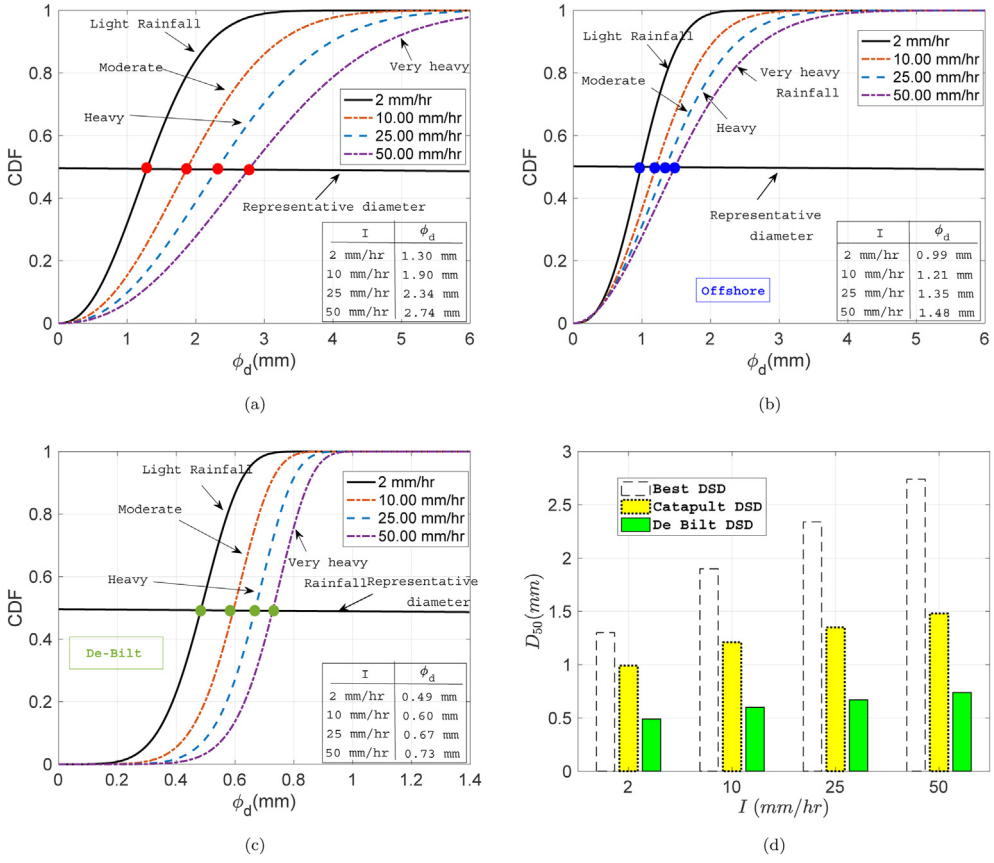

Fig. 12. Comparison of DSDs for different rainfall conditions with representative I (a) Best's DSD (b) Catapult's DSD (c) De Bilt's DSD (d) comparison of D_{50} for different DSD.

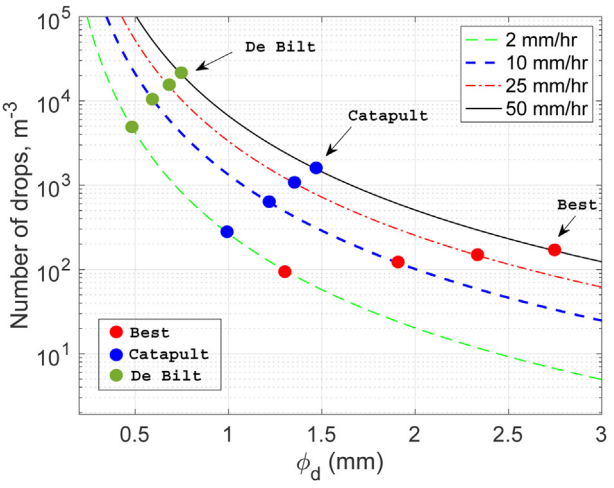

Fig. 13. Comparison of number of drops for different I and φ_d with different DSD.

which are tabulated in Table 6. These seasonal DSDs are useful when a detailed analysis of LEE or development of erosion safe control algorithm is required to be performed more specifically applied to specific seasons. Nevertheless, it is observed from the figure that there is not much seasonal difference in the parameters representing the DSD. Hence, in the rest of the discussion, reference to only non-seasonal DSD will be made.

Table 6
Constants determined for seasonal DSD at the De Bilt site.

Constants Season	A	p	N	q
Winter	0.4690	0.1411	4.522	0.1402
Spring	0.5175	0.1044	5.0480	0.1697
Summer	0.5046	0.1134	4.4238	0.2244
Autumn	0.4625	0.1186	4.3623	0.2144

6.2. Marginal distribution of rainfall intensity $f_I(I)$

For determining the best fit for marginal distribution of rainfall intensity, hourly rainfall intensity data for inland De Bilt site as well as the coastal site De Kooy De Bilt site are plotted on $Q-Q$ plots of both lognormal and gamma distributions. Fig. 15(a) presents $Q-Q$ plot with data representing De Bilt site.

It can be seen from the figure that the lognormal distribution is a more suitable fit for the rainfall intensity as the data is relatively closer to the straight line. A similar observation is found for the De Kooy site where the lognormal distribution was obtained as a more suitable distribution fit to represent the rainfall intensity. Nevertheless, the distribution parameters for lognormal (μ and σ) and gamma distributions (a and b) are obtained usingMaximum Likelihood Estimation (MLE) method for both the sites and is summarised in Table 7. Fig. 15(b) compares the histogram data representing the rainfall intensity for the De Bilt site with the fitted lognormal and gamma distribution based on the parameters estimated in Table 7. The results show that the gamma distribution under predicts the low rainfall intensity, whereas lognormal

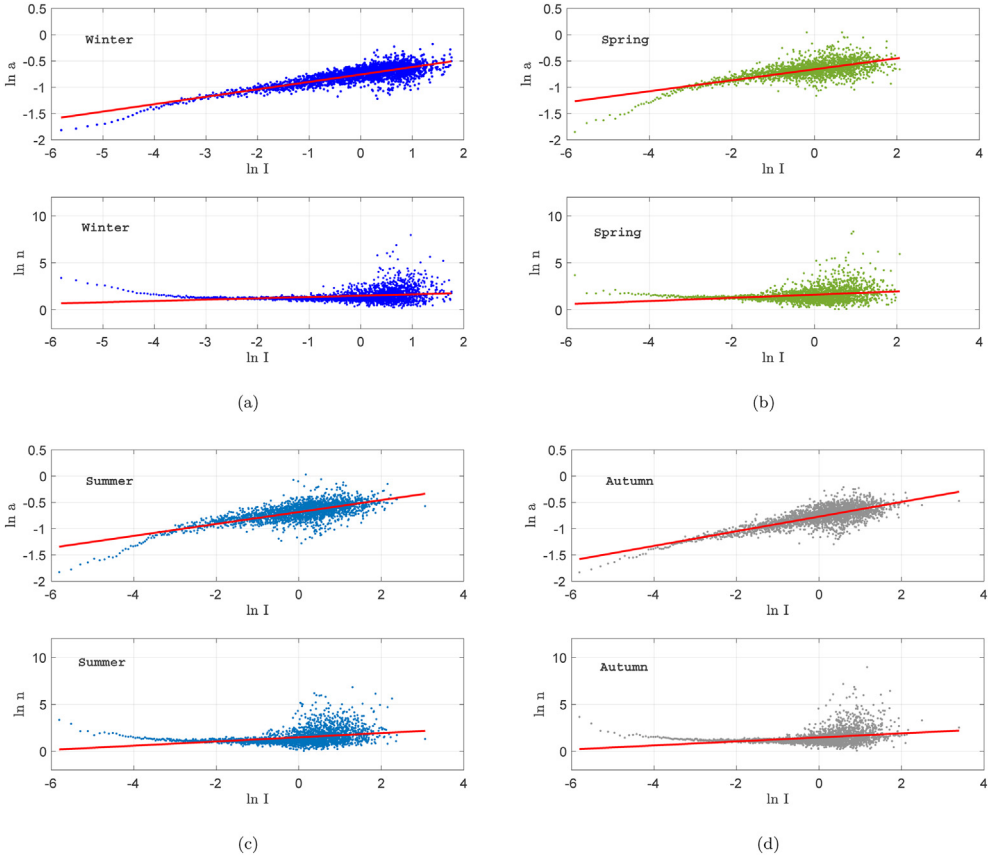

Fig. 14. Calculation of constants A, p, N and q for (a) Winter (b) Spring (c) Summer (d) Autumn seasonal DSD.

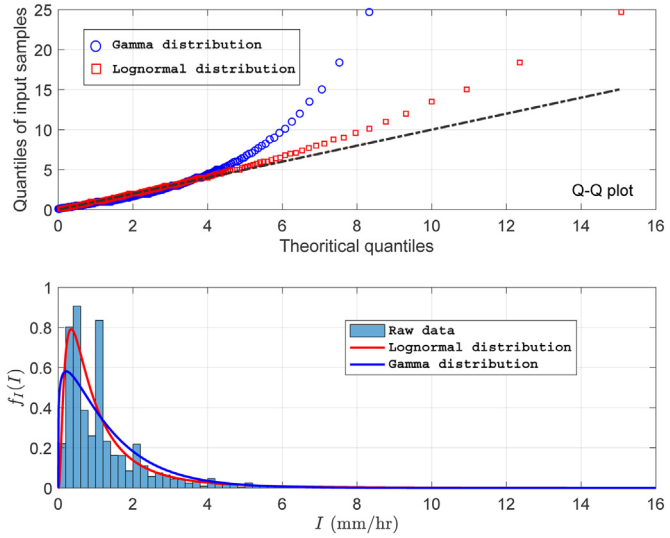

Fig. 15. (a) Comparison of $Q-Q$ plots for lognormal and gamma for describing I (b) Comparison of raw data with lognomral and gamma marginal distribution.

Table 7
Distribution parameter for lognormal and gamma for I at De Bilt and De Kooy site.

Parameter Site	μ	σ	a	b
1. De Bilt	−0.1816	0.8617	1.912	1.126
2. De Kooy	−0.1445	0.8275	1.2765	1.0531

distribution slightly underestimates the higher rain intensity. A χ^2 goodness of fit test was considered and it was found that lognormal distribution cannot be rejected at 5% significance level. A comparison of the empirical CDF and lognormal CDF for the rainfall intensity is presented in Fig. 16(a)-(b) and relatively higher differences can be seen for the case of gamma distribution compared to the lognormal distribution. Overall, the rainfall intensity (I) is found to be best described by lognormal distribution for both the sites.

6.3. Percentage of rain duration for different intensities (P(I))

Table 8 compares $P(I)$ for the inland and coastal sites for different classes of rain intensities. It is seen that the percentage of dry periods at both the sites is more than 88% of the total time based on fifty years of hourly data. Also, most of the rainfall falls under the light rainfall conditions category for both the sites (0.05 mm/h $\leq I < 2.5$ mm/h) whereas moderate, heavy and very heavy rainfall conditions are quite rare in realistic conditions and

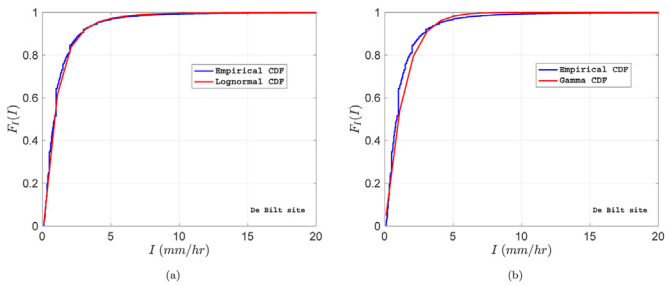

Fig. 16. Comparison of emperical CDF with (a) lognormal CDF (b) gamma PDF for representing I.

Table 8
$P(I)$ calculated for different type of rainfall for De Bilt and De Kooy site.

Type of rainfall	Range of intensity	De Bilt P(I)%	De Kooy P(I)%
No rainfall	$I < 0.05$	88.26	88.47
Light rainfall	$0.05 \leq I < 2.5$	10.29	10.08
Moderate rainfall	$2.5 \leq I < 10$	1.35	1.364
Heavy rainfall	$10 \leq I < 50$	0.0910	0.0801
Very heavy rainfall	$I \geq 50$	0.00069	0.00046

only account for less than 2% of the total rainfall time. It was also observed that the percentage of rain duration for different classes of rain intensities are similar at both the sites (see Table 8).

6.4. Joint probability distribution of rainfall intensity and rain droplet size ($f_{I,\varphi_d}(I,\varphi_d)$)

A comparison of the joint PDF of rainfall intensity and rain droplet size for inland as well as the coastal site is presented through Figs. 17-18. For the inland De Bilt site, the joint PDF is determined by combining the marginal distribution of I representing the De Bilt site with De Bilt's DSD (Fig. 17(a)). Moreover, in order to check the sensitivity of the joint PDF to the choice of DSD, the marginal distribution of I for the De Bilt site is also further combined with Best's DSD (Fig. 17(b)), which is one of the most commonly applied onshore DSD in the literature. On the other hand, for the coastal De Kooy site (Fig. 18), the joint PDF is determined by combining the marginal distribution of I corresponding to the De Kooy site with Catapult's DSD that represent offshore rainfall. There are some important observations that can be made for the joint PDF from these figures: (a) for both the sites, the joint PDF clearly shows the dominance of light rainfall conditions at the site ($I < 2.5$ mm/h), however, there are differences in the corresponding rain droplet size depending upon the DSD used (b) the joint PDF for the inland onshore site varies for De Bilt's and Best's DSD. For instance, the joint PDF for the site with De Bilt's DSD shows dominance of droplet size less than 0.6 mm (Fig. 17(a)), whereas for Best's DSD, the dominance of droplet size ranges till 2 mm (Fig. 17(b)). As a result, the probabilistic rainfall model is highly sensitive to the choice of DSD. (c) The joint PDF of coastal site shows a slightly larger occurrence of rainfall intensity above 2 mm/h, and corresponding smaller droplet size compared to the joint PDF considered with Best's DSD.

6.5. Application and case studies

6.5.1. Marginal distribution of mean wind speed ($f(U_w)$)

The case study considers NREL 5 MW reference turbine as the base case which has a hub height of 90 m. During the precipitation, the impact of rain droplets with the rotating blade is dominated by the blade tip speed which depends upon the expected mean wind speed at the hub height. The hourly mean wind speed data for both the sites are available at 10 m reference height, and is extrapolated to 90 m hub height using the power law. The extrapolated dataset is then fitted to lognormal and Weibull $Q-Q$ plot to check the appropriateness of the considered distribution (Fig. 19(a)-(b)). The results show that Weibull distribution provides a more appropriate fit than the lognormal, as the data points are close to the straight line in the case of Weibull distribution. Further, the coefficient of determination and standard error are checked and it was confirmed that the mean wind speed for both the sites are well described by Weibull distribution.

Moreover, the distribution parameters for two parameter Weibull distribution for both the sites are obtained using the Maximum

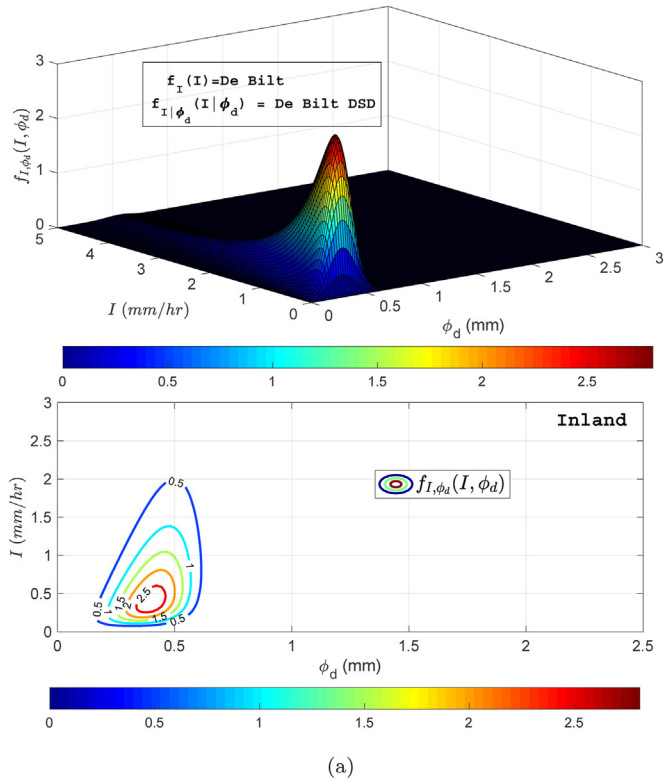

(a)

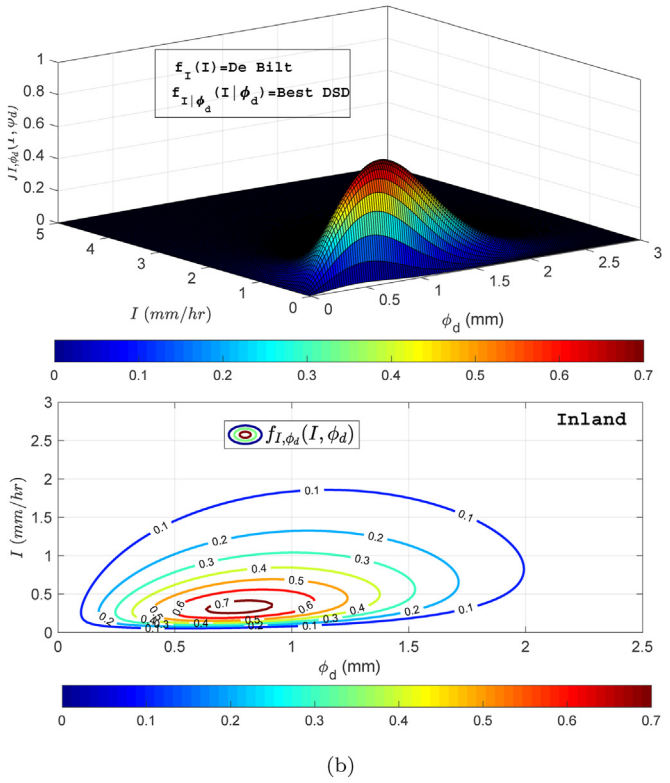

(b)

Fig. 17. Joint PDF ($f_{\varphi_d|I}(\varphi_d|I)$) for inland De Bilt site with (a) De Bilt's DSD (b) Best's DSD.

Likelihood Estimation (MLE) method (α_u: shape parameter and β_u: scale parameter) and are tabulated in Table 9. Fig. 19(c)–(d) present the marginal PDF for the mean wind speed at the hub height for both the sites and it can be seen that the average wind speed as well

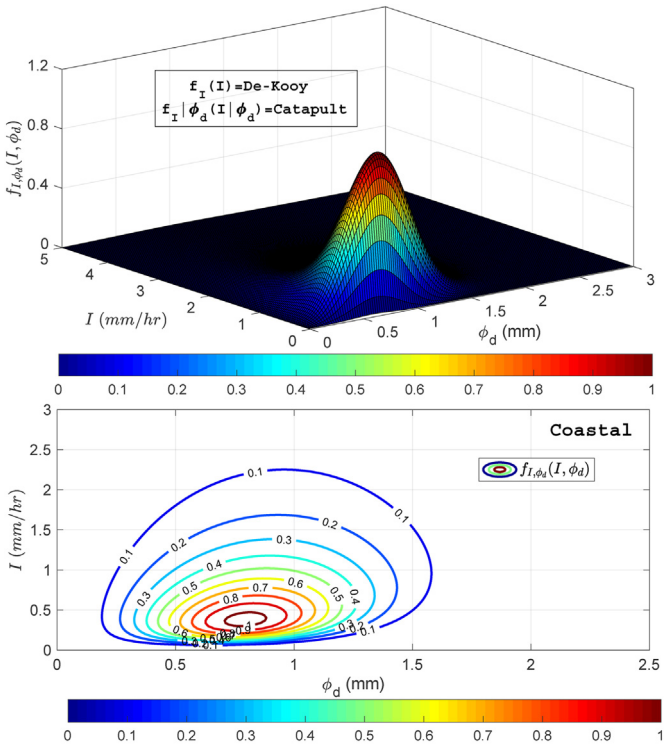

(a)

Fig. 18. Joint PDF ($f_{\varphi_d|I}(\varphi_d|I)$) for coastal De Kooy site with Catapult's DSD.

as the shape parameter (β_u) at the coastal site is comparatively higher than the inland site. This is in line with the general observation about the preference for installing turbines in coastal and offshore environments for efficient power production.

6.5.2. *Estimation of erosion damage rates and expected life of the blade coating*

Fig. 20(a) presents the short term erosion damage rate of the blade coating ($\dot{D}_i^{ST}(I, \varphi_d, U_w)$) calculated for the rotating WTB for different rainfall conditions at the rated wind speed. The comparison is presented in the figure for erosion damage rate calculated by considering rainfall scenario through De Bilt's and Best's DSD for the inland site, and by considering Catapult's DSD for the coastal site. Note that these figures do not include the probability of occurrence of given rain and wind conditions as well as the dry periods of rainfall and represents coating damage under accelerated erosion. The only difference by choosing different DSDs is the difference in the median droplet size for different representative rainfall types (see Fig. 12(d) for reference). There are two important observations from the figure: (1) For any given DSD, the erosion damage rate increases with increasing rainfall intensity and is largest for very heavy rainfall condition ($I = 50$ mm/h). On the other hand, for any given rainfall type, the erosion damage rate is largest for rainfall scenario described by De Bilt's DSD, followed by Catapult's offshore DSD and the least is for Best's DSD. One of the important reasons for this is the fact that De Bilt's DSD predicts a smaller droplet radius for the given rainfall intensity, and therefore there are a large number of droplets in the same volume of rain that will hit the blade during rotation, compared to the coastal site described by Catapult and the inland site described by Best's DSD. In other words, among different DSDs considered in the paper, Best's DSD seems to underpredict the acclerated erosion damage

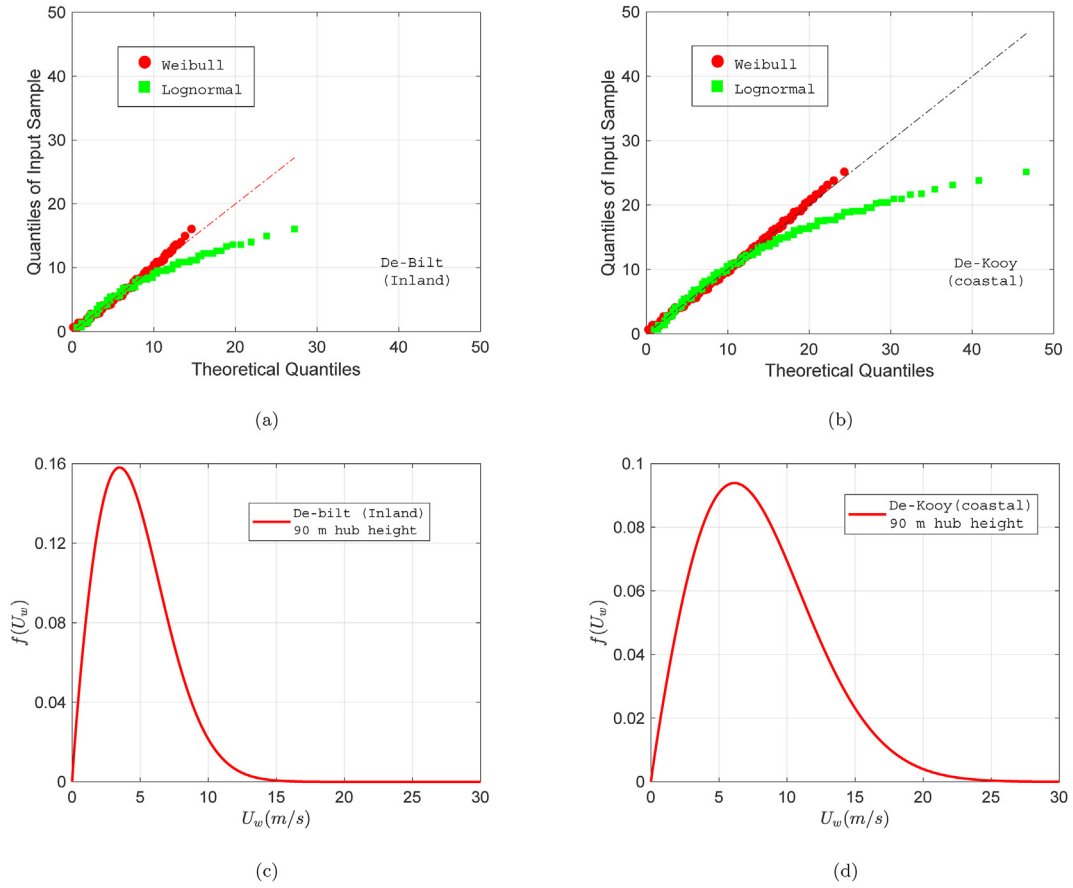

Fig. 19. Comparison of $Q-Q$ plot between lognormal and Weibull distribution for: (a) inbilt De Bilt site (b) De Kooy coastal site; Comparison of $f(U_w)$ at 90 m hub height (c) inbilt De Bilt site (d) De Kooy coastal site.

Table 9
Weibull distribution parameter for the site De Bilt and De Kooy.

Parameter Site	α_u	β_u
1. De Bilt	1.8763	5.2162
2. De Kooy	1.9331	8.9419

rate of the coating, indicating an overprediction in the estimate of coating lifetime.

It is to be noted that the above results do not completely describe the realistic coating degradation rate of a WTB during the service life, as the results do not include probability of occurrence of rain and wind conditions at the wind turbine site. Therefore, *probabilistic erosion damage rate* ($\dot{D}_i^P(I, \varphi_d, U_w)$) is calculated by combining the short term erosion damage rate for the WTB with corresponding probability of occurrence of considered rain and wind conditions. Fig. 20(b)–(f) present the probabilistic erosion damage rate ($\dot{D}_i^P(I, \varphi_d, U_w)$) for different rainfall types and different range of wind speeds. The rainfall condition at the inland De Bilt site is described by De Bilt's DSD as well as Best's DSD whereas the rainfall condition at the coastal site is described by Catapult's DSD. In these figures, different operational U_w are considered, for instance (U_w = 6 m/s) represents below rated wind speed, (U_w = 13 m/s U_w = 16 m/s 20 m/s) represents above rated wind speed, and (U_w = 24 m/s) is close to the cut-off wind speed. It can be seen from all the figures that the most dominating rainfall type that causes the largest erosion damage rate of the blade coating belongs to the category of light rainfall conditions ($I \leq 2.5$ mm/h). This is due to the fact that light rainfall conditions have the highest probability of occurrence for both the sites. In addition, there is significantly less erosion damage rate during heavy rainfall conditions, as their occurrence rate is associated with a very small probability. Also, as the mean wind speed increases and shifts away from the rated wind speed and approaches the cut-off range, the erosion damage rate increases significantly for the coastal site compared to the inland site. This is due to the fact that the marginal mean wind speed distribution for the coastal site considered in the paper has a higher probability of occurrence of U_w above rated conditions compared to the inland site. Overall, mean wind speed (U_w) together with rain intensity (I) plays a crucial role during the leading-edge erosion analysis. Also, as discussed before, among different DSDs considered, Best's DSD seems to underpredict the erosion damage rate of coating, and this implies overprediction of the coating life.

Finally, the *long term erosion damage rate* and the expected life of the blade coating is calculated by performing a weighted sum of short term erosion damage rate for all possible rain and wind conditions that can occur at the site during the blade's service life together with their probability of occurrence. Fig. 21 compares the expected lifetime of the blade coating for the inland and the coastal site. The expected life of the blade coating system is found to be less for the coastal De Kooy site compared to the inland De Bilt site. The expected life is obtained as 4.2 years for the inland site compared to the expected life of 1.2 years for the coastal site. One of the important reasons that contributes to the accelerated erosion at the coastal site is that the probability of occurrence of wind speed between rated and cut-off conditions is higher at the coastal site

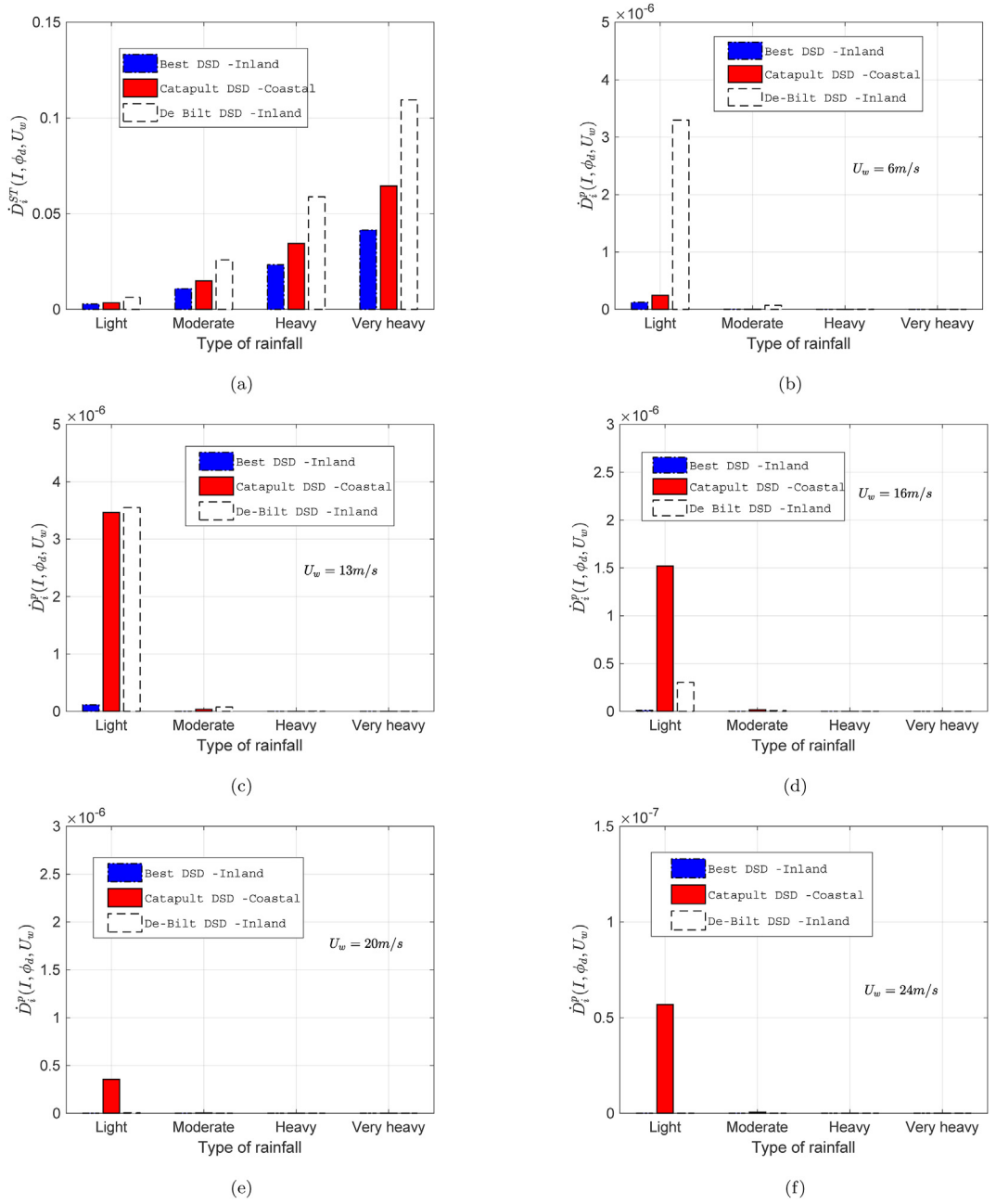

Fig. 20. (a) Comparison of short term damage erosion rate ($\dot{D}_i^{ST}(I,\varphi_d,U_w)$) for different rainfall conditions, inland and coastal sites and their associated DSDs; probabilistic damage erosion rate ($\dot{D}_i^{P}(I,\varphi_d,U_w)$) for different rainfall types (b) U_w = 6 m/s,(c) U_w = 13 m/s (d) U_w = 16 m/s (e) U_w = 20 m/s,(f) U_w = 24 m/s.

compared to the inland site. For instance, Fig. 22 compares the exceedance probability of rated wind speed for both the sites and it can be clearly seen that the point where the black dotted line intersects the curve has a larger probability of exceedance for the coastal site. The blade rotation in this regime is expected to cause the highest erosion damage rate, given that it is associated with the highest blade tip speed during blade rotation. In this way, blade rotates at the rated speed for a large period of time and erodes relatively faster during precipitation at the coastal site compared to the inland site. The finding is also in line with the industrial experience and observations found in the literature [14,25] where the expected life of blade in offshore and coastal regions is found to be less compared to the inland site.

In all the above discussions, hourly rain and wind statistic corresponding to fifty years of data were considered for the development and application of probabilistic rainfall model to estimate leading-edge lifetime of the blade coating. However, on many occasions the availability of the length of data is limited and varies from site to site. A sensitivity study is performed to check the effect of the data period on the expected life of the coating calculated for inland and coastal sites. All the calculations performed in the paper are repeated for different data periods ranging from 50 years to 2 years and the expected life of the blade coating is evaluated. Fig. 23 compares the expected life of the coating system calculated for inland and coastal sites and corresponds to the data periods of 50 years, 25 years, 10 years and 2 years. The results for the coating lifetime are found consistent with varying data periods, with a longer expected life estimated for the inland De Bilt site compared to the coastal site.

Also, the magnitudes of the expected life of the coating are in

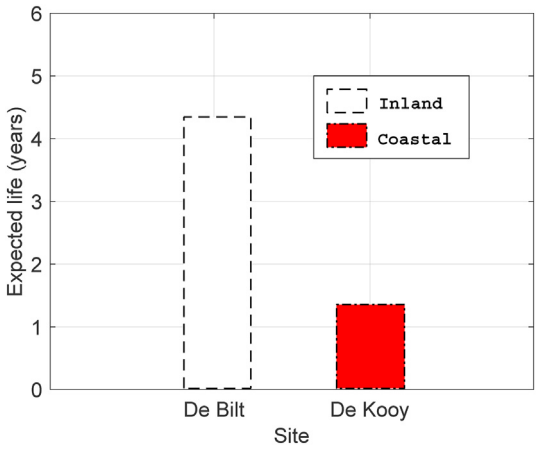

Fig. 21. Calculation of expected life of the blade coating for the inland De Bilt and coastal De Kooy site.

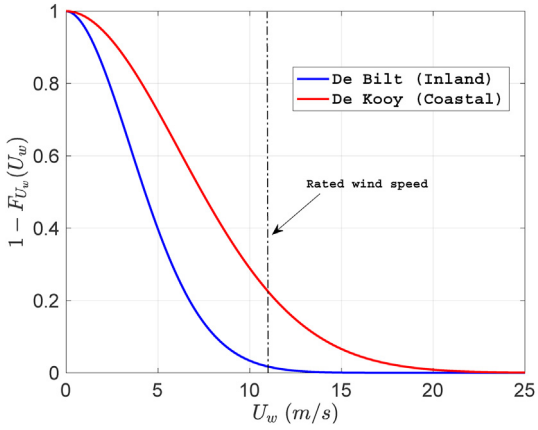

Fig. 22. Comparison of exceedance probability of wind speed for for the inland De Bilt and coastal De Kooy site.

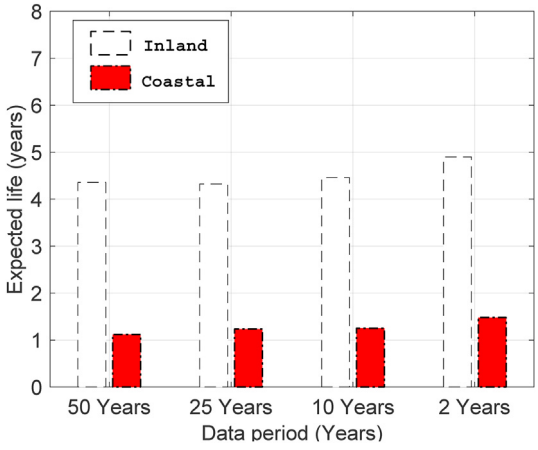

Fig. 23. Calculation of expected life of the blade coating for the inland De Bilt and coastal De Kooy site by considering different data period of measurement.

close agreement for different data periods with differences between estimates using 50, 25 and 10 years of data being less than 5%, and the difference between estimates using 50 and 2 years of data period being around 10%. These results confirm our initial hypothesis that the probabilistic distribution of the rainfall parameters is a consistent input form for the rainfall statistic model to determine the leading-edge lifetime of blade coating system. In addition, the expected life estimated using the model for both coastal (1.2 *years*) and inland site (4.2 *years*) falls within the range of values seen insitu [25,36] which verifies the performance of the proposed model.

7. Conclusions

The present paper proposed a probabilistic rainfall model that enables site-specific assessment of leading-edge lifetime of the blade coating system through the probabilistic distributions of rain and wind conditions for a given wind turbine site. An application of the proposed model was presented through case studies for a 5 MW wind turbine. The analytical surface fatigue model from Springer [29] was coupled with the rainfall statistic and the wind turbine model. The expected lifetime of the blade coating was compared for both inland and coastal sites using a long-term probabilistic assessment. Following are the main conclusions:

1. A new droplet size distribution (DSD) was determined based on two years of onshore rainfall data measured by KNMI using the Thies Clima disdrometer at the inland De Bilt site in the Netherlands which has the form:

$$F_{\varphi_d|I}(\varphi_d|I) = 1 - exp\left[- \left(\frac{\varphi_d}{0.4811 \cdot I^{0.1186}} \right)^{4.56 \cdot I^{0.14}} \right] \tag{29}$$

2. The proposed DSD was compared with the most frequently used DSD from the literature i.e. Best's DSD [38] as well as Catapult's DSD [40] where the later represent offshore rainfall. It was found that there is a large deviation in the statistical representation of the rain droplet size by these DSDs and the difference increases with increasing I. A quantitative comparison for median droplet size (D_{50}) between DSDs showed that for all the cases D_{50} increases with increasing I. However, Best's DSD was found to overestimate the D_{50} among all the three DSDs. For instance, D_{50} for Best's distribution was 2.74 mm for $I = 50$ mm/h, whereas for Catapult's DSD it was 1.48 mm, and for De Bilt's DSD the median droplet size was 0.73 mm.
3. The differences in the estimates of D_{50} by different DSDs was also reflected in the number of droplets ($\bar{q}$) that could occur in the rainfall for a given I. This was due to the fact that $\bar{q}$ is inversely proportional to cube of droplet size (see eq. (21)). The results showed that the number of drops are significantly larger for the same amount of rain for De Bilt's DSD compared to Catapult's DSD and Best's DSD.
4. Next, the marginal distribution of the rainfall intensity together with the mean wind speed were established for the above stated inland as well as the coastal De Kooy site and their distribution parameters were obtained. The lognormal distribution was found to be the best fit for the rainfall intensity, whereas Weibull distribution was found as the best fit for the marginal wind speed at the hub height for both the sites.
5. A comparison of percentage of rain duration for different intensities ($P(I)$) was compared for the inland De Bilt as well as the coastal De Kooy site. It was found that the percentage of dry periods is more than 88% of the total time based on fifty years of hourly data for both the sites. Further, the $P(I)$ for different rainfall categories at both the sites were nearly similar. On the other hand, with regards to mean wind speed, it was found that

the average wind speed at the hub is comparatively higher at the coastal site than at the inland site.

6. The joint PDF of I and φ_d for the inland site and the coastal site was presented and compared. It was found that for both the sites, the joint PDF showed the dominance of light rainfall conditions (I < 2.5 mm/h). However with varying DSDs, the probability of the occurrence of corresponding droplet size varied. For instance, the joint PDF for the inland site with De Bilt's DSD showed dominance of droplet size less than 0.6 mm, whereas for Best's DSD, the dominance of droplet size ranged till 2 mm. As a result, the probabilistic rainfall model was found highly sensitive to the choice of DSD.
7. Finally, a long term erosion damage rate and the expected life of the blade coating were calculated by performing a weighted sum of short term erosion damage rate for all the possible rain and wind conditions that can occur at the site during the blade's service life together with their probability of occurrence. The expected life of the blade coating system was found to be less for the coastal De Kooy site (1.2 *years*) compared to the inland De Bilt site (4.2 *years*). One of the primary reasons that contributed to the accelerated erosion at the coastal site is the higher probability of occurrence of mean wind speed between rated and cut-off conditions for the turbine compared to the inland site. Also, the estimated erosion damage rate was found consistent with varying data periods used for the analysis.

8. Limitation and recommendation for future work

The present paper established a framework for a probabilistic rainfall model that can be fed to an LEE model to determine the expected life of the blade coating. However, there are some simplifications and limitations associated with the current work which presents scope for future work.

In the paper, a few assumptions were made to estimate the expected leading-edge lifetime of blade coating system. In the analysis, it was assumed that wind turbine is operating at all times between the cut-in and cut-off wind conditions. However, in reality, there may be some downtime already due to inspection and repair of other equipment of the wind turbines and thus the results are conservative. These factors need to be considered in the future.

For estimating the leading-edge lifetime, the Springer's model for homogeneous coating system was considered, and effect of substrate below the coating was ignored. This was based on the industrial interaction where it was mentioned that for the given coating considered in the work, material degradation at the surface is the governing problem. In the future work, the effects of composite substrates below the coating will be included in the analysis.

In the paper, two different sites - an inland De Bilt and coastal De Kooy - were considered. However, it was only for the De Bilt site for which the DSD was estimated and later combined with the site's marginal distribution of rain intensity to obtain the joint PDF of I and φ_d. However, for obtaining the joint PDF for the De Kooy site, the Catapult's offshore DSD was used along with the site's marginal distribution of rain intensity. There are no disdrometer measurements available for the coastal De Kooy site or for offshore conditions. In the future, more disdrometer measurements will be obtained to perform similar analysis for different onshore and offshore wind turbine sites in the Netherlands.

In the paper, the wind speed (U_w) and rainfall intensity (I) were considered as independent random variables, however, in general U_w and I can also be described by a joint PDF according to Ref. [62]. In this way, it will be possible to obtain more accurate results where the long term assessment will include probability of simultaneous occurrence of mean wind speed and rain intensity.

Also, in the current study, the analytical surface fatigue model from Ref. [29] was used along with one particular coating used in the industry. A parametric study will be performed in the future with different erosion models available in the literature along with different coating materials to rank the performance of models as well as coatings. For this it will also be essential to validate the results with the insitu observations.

CRediT authorship contribution statement

Amrit Shankar Verma: proposed the, Methodology, Writing – original draft, conducted the simulations, and wrote the paper. **Zhiyu Jiang:** discussed the paper, reviewed the rebuttal, and revised the manuscript. **Marco Caboni:** provided the disdrometer dataset for the site, discussed the paper and revised the manuscript. **Hans Verhoef:** provided the disdrometer dataset for the site, discussed the paper and revised the manuscript. **Harald van der Mijle Meijer:** provided the disdrometer dataset for the site, discussed the paper and revised the manuscript. **Saullo G.P. Castro:** Writing – review & editing, discussed the paper, reviewed the rebuttal, and revised the manuscript. **Julie J.E. Teuwen:** Writing – review & editing, discussed the paper, reviewed the rebuttal, and revised the manuscript.

Declaration of competing interest

The authors declare that they have no known competing financial interests or personal relationships that could have appeared to influence the work reported in this paper.

Acknowledgment

This work was made possible through the WINDCORE project having subsidy scheme TSE–18–04–01–Renewable energy project with project number TEHE118013. Authors highly appreciate the financial support. The authors also appreciate the in-kind support of consortium partners in the WINDCORE project for their discussions which helped us to improve the quality of our work.

References

[1] E.W.E. Association, et al., EU Energy Policy to 2050, EWEA, 2011.
[2] I. Pineda, P. Tardieu, The European Offshore Wind Industry – Key Trends and Statistics, 2016. https://windeurope.org/. Accessed: -06-01).
[3] A.S. Verma, Z. Jiang, N.P. Vedvik, Z. Gao, Z. Ren, Impact assessment of a wind turbine blade root during an offshore mating process, Eng. Struct. 180 (2019) 205–222.
[4] K. Pugh, G. Rasool, M.M. Stack, Raindrop erosion of composite materials: some views on the effect of bending stress on erosion mechanisms, Journal of Bio- and Tribo-Corrosion 5 (2) (2019) 45.
[5] A.S. Verma, S.G. Castro, Z. Jiang, J.J. Teuwen, Numerical investigation of rain droplet impact on offshore wind turbine blades under different rainfall conditions: a parametric study, Compos. Struct. (2020) 112096.
[6] M.H. Keegan, D. Nash, M. Stack, Modelling rain drop impact on offshore wind turbine blades, ASME Turbo Expo (Proceedings of the TURBO EXPO 2012 GT2012 June 11-15, 2012, Copenhagen, Denmark) (2012) (2012) Article–GT.
[7] M.H. Keegan, D. Nash, M. Stack, Wind Turbine Blade Leading Edge Erosion: an Investigation of Rain Droplet and Hailstone Impact Induced Damage Mechanisms, Ph.D. thesis, University of Strathclyde, 2014.
[8] Leon. Mishnaevsky Jr., Toolbox for optimizing anti-erosion protective coatings of wind turbine blades: overview of mechanisms and technical solutions, Wind Energy 22 11 (2019) 1636–1653.
[9] W. Han, J. Kim, B. Kim, Effects of contamination and erosion at the leading edge of blade tip airfoils on the annual energy production of wind turbines, Renew. Energy 115 (2018) 817–823.
[10] R. Herring, K. Dyer, F. Martin, C. Ward, The increasing importance of leading edge erosion and a review of existing protection solutions, Renew. Sustain. Energy Rev. 115 (2019) 109382.
[11] R. Wiser, K. Jenni, J. Seel, E. Baker, M. Hand, E. Lantz, A. Smith, Forecasting Wind Energy Costs and Cost Drivers: the Views of the World's Leading Experts.
[12] https://www.armouredge.com/, (Picture taken).

[13] Picture taken under permission from TNO, https://www.tno.nl.
[14] C. Hasager, F. Vejen, J. Bech, W. Skrzypiński, A.-M. Tilg, M. Nielsen, Assessment of the rain and wind climate with focus on wind turbine blade leading edge erosion rate and expected lifetime in Danish seas, Renew. Energy 149 (2020) 91–102.
[15] E. Cortés, F. Sánchez, L. Domenech, A. Olivares, T. Young, A. O'Carroll, F. Chinesta, Manufacturing issues which affect coating erosion performance in wind turbine blades, in: AIP Conference Proceedings, vol. 1896, AIP Publishing, 2017, 030023.
[16] E. Cortés, F. Sánchez, A. O'Carroll, B. Madramany, M. Hardiman, T. Young, On the material characterisation of wind turbine blade coatings: the effect of interphase coating–laminate adhesion on rain erosion performance, Materials 10 (10) (2017) 1146.
[17] H. Slot, E. Gelinck, C. Rentrop, E. Van Der Heide, Leading edge erosion of coated wind turbine blades: review of coating life models, Renew. Energy 80 (2015) 837–848.
[18] H. Slot, R. IJzerman, M. le Feber, K. Nord-Varhaug, E. van der Heide, Rain erosion resistance of injection moulded and compression moulded polybutylene terephthalate pbt, Wear 414 (2018) 234–242.
[19] A. Fraisse, J.I. Bech, K.K. Borum, V. Fedorov, N.F.-J. Johansen, M. McGugan, L. Mishnaevsky Jr., Y. Kusano, Impact fatigue damage of coated glass fibre reinforced polymer laminate, Renew. Energy 126 (2018) 1102–1112.
[20] L. Bartolomé, J. Teuwen, Prospective challenges in the experimentation of the rain erosion on the leading edge of wind turbine blades, Wind Energy 22 (1) (2019) 140–151.
[21] M.H. Keegan, D. Nash, M. Stack, On erosion issues associated with the leading edge of wind turbine blades, J. Phys. Appl. Phys. 46 (38) (2013) 383001.
[22] B. Astrid, Investigation of droplet erosion for offshore wind turbine blades, Ann. Acad. Med. Stetin 59 (1) (2014) 170–171.
[23] A. Castorrini, A. Corsini, F. Rispoli, P. Venturini, K. Takizawa, T.E. Tezduyar, Computational analysis of wind-turbine blade rain erosion, Comput. Fluids 141 (2016) 175–183.
[24] A. Corsini, A. Castorrini, E. Morei, F. Rispoli, F. Sciulli, P. Venturini, Modeling of Rain Drop Erosion in a Multi-Mw Wind Turbine, ASME Paper No. GT2015-42174.
[25] B. Amirzadeh, A. Louhghalam, M. Raessi, M. Tootkaboni, A computational framework for the analysis of rain-induced erosion in wind turbine blades, part ii: drop impact-induced stresses and blade coating fatigue life, J. Wind Eng. Ind. Aerod. 163 (2017) 44–54.
[26] B. Amirzadeh, A. Louhghalam, M. Raessi, M. Tootkaboni, A computational framework for the analysis of rain-induced erosion in wind turbine blades, part i: stochastic rain texture model and drop impact simulations, J. Wind Eng. Ind. Aerod. 163 (2017) 33–43.
[27] W. Hu, W. Chen, X. Wang, Z. Jiang, Y. Wang, A.S. Verma, J.J. Teuwen, A computational framework for coating fatigue analysis of wind turbine blades due to rain erosion, Renew. Energy 170 (2021) 236–250.
[28] Leon Doagou-RadSaeedMishnaevsky Jr., I. Bech Jakob, Leading edge erosion of wind turbine blades: Multiaxial critical plane fatigue model of coating degradation under random liquid impacts, Wind Energy 23 (8) (2020) 1752–1766.
[29] G. S. Springer, Erosion by Liquid Impact.
[30] B.-E. Lee, K.-J. Riu, S.-H. Shin, S.-B. Kwon, Development of a water droplet erosion model for large steam turbine blades, KSME Int. J. 17 (1) (2003) 114–121.
[31] C. B. Burson-Thomas, R. Wellman, T. J. Harvey, R. J. Wood, Importance of surface curvature in modeling droplet impingement on fan blades, J. Eng. Gas Turbines Power 141 (3).
[32] G.S. Springer, C.I. Yang, Optical transmission losses in materials due to repeated impacts of liquid droplets, AIAA J. 13 (11) (1975) 1483–1487.
[33] G.S. Springer, C. Baxil, A model for rain erosion of homogeneous materials, in: Erosion, Wear, and Interfaces with Corrosion, ASTM International, 1974.
[34] G.S. Springer, C.-I. Yang, P.S. Larsen, Analysis of rain erosion of coated materials, J. Compos. Mater. 8 (3) (1974) 229–252.
[35] G.S. Springer, C.I. Yang, Model for the rain erosion of fiber reinforced composites, AIAA J. 13 (7) (1975) 877–883.
[36] D. Eisenberg, S. Laustsen, J. Stege, Wind turbine blade coating leading edge rain erosion model: development and validation, Wind Energy 21 (10) (2018) 942–951.
[37] Jakob BechIlsted, Charlotte Bay Hasager, Bak Christian, Extending the life of wind turbine blade leading edges by reducing the tip speed during extreme precipitation events, Wind Energy Science 3 (2) (2018) 729–748.
[38] A. Best, The size distribution of raindrops, Q. J. R. Meteorol. Soc. 76 (327) (1950) 16–36.
[39] J.S. Marshall, W.M.K. Palmer, The distribution of raindrops with size, J. Meteorol. 5 (4) (1948) 165–166.
[40] R. Herring, K. Dyer, P. Howkins, C. Ward, Characterisation of the offshore precipitation environment to help combat leading edge erosion of wind turbine blades, Wind Energy Science Discussions (2020) 1–16, https://doi.org/10.5194/wes-2020-11, 2020.
[41] N.C. Dzupire, P. Ngare, L. Odongo, A Poisson-gamma model for zero inflated rainfall data, Journal of Probability and Statistics (2018), https://doi.org/10.1155/2018/1012647.
[42] B. Kedem, H. Pavlopoulos, X. Guan, D.A. Short, A probability distribution model for rain rate, J. Appl. Meteorol. 33 (12) (1994) 1486–1493.
[43] H.-K. Cho, K.P. Bowman, G.R. North, A comparison of gamma and lognormal distributions for characterizing satellite rain rates from the tropical rainfall measuring mission, J. Appl. Meteorol. 43 (11) (2004) 1586–1597.
[44] D. Salisu, S. Supiah, A. Azmi, et al., Modeling the distribution of rainfall intensity using hourly data, Am. J. Environ. Sci. 6 (3) (2010) 238–243.
[45] S. Adiku, P. Dayananda, C. Rose, G. Dowuona, An analysis of the within-season rainfall characteristics and simulation of the daily rainfall in two savanna zones in Ghana, Agric. For. Meteorol. 86 (1–2) (1997) 51–62.
[46] J.O. Laws, D.A. Parsons, The relation of raindrop-size to intensity, Eos, Trans. Am. Geophys. Union 24 (2) (1943) 452–460.
[47] R. Acharya, Satellite Signal Propagation, Impairments and Mitigation, Academic Press, 2017.
[48] D. Deirmendjian, Electromagnetic Scattering on Spherical Polydispersions, Tech. Rep., Rand Corp Santa Monica CA, 1969.
[49] A. Zainal, I. Glover, P. Watson, Rain rate and drop size distribution measurements in Malaysia, in: Proceedings of IGARSS'93-IEEE International Geoscience and Remote Sensing Symposium, IEEE, 1993, pp. 309–311.
[50] https://www.knmi.nl, (Picture).
[51] A.S. Verma, Z. Jiang, Z. Ren, Z. Gao, N.P. Vedvik, Response-based assessment of operational limits for mating blades on monopile-type offshore wind turbines, Energies 12 (10) (2019) 1867.
[52] A.S. Verma, Z. Gao, Z. Jiang, Z. Ren, N.P. Vedvik, Structural safety assessment of marine operations from a long-term perspective: a case study of offshore wind turbine blade installation, in: ASME 2019 38th International Conference on Ocean, Offshore and Arctic Engineering, American Society of Mechanical Engineers Digital Collection, 2019.
[53] L. Li, Z. Gao, T. Moan, Joint distribution of environmental condition at five european offshore sites for design of combined wind and wave energy devices, J. Offshore Mech. Arctic Eng. 137 (3) (2015), 031901.
[54] A. Overeem, Climatology of Extreme Rainfall from Rain Gauges and Weather Radar, 2009.
[55] M.K. Ochi, Applied Probability and Stochastic Processes: in Engineering and Physical Sciences, vol. 226, Wiley-Interscience, 1990.
[56] J. Jonkman, S. Butterfield, W. Musial, G. Scott, reportDefinition of a 5-mw Reference Wind Turbine for Offshore System Development, National Renewable Energy Laboratory, Golden, CO, Technical Report No. NREL/TP-500-38060.
[57] I. 61400-3, Wind Turbines, Part 3: Design Requirements for Offshore Wind Turbines, 2009.
[58] D. Atlas, R. Srivastava, R.S. Sekhon, Doppler radar characteristics of precipitation at vertical incidence, Rev. Geophys. 11 (1) (1973) 1–35.
[59] S.S. Sandbakken, Long Term Analysis of Semi Submersible Offset, Master's thesis, NTNU, 2016.
[60] https://multimedia.3m.com/mws/media/978868O/3m-wind-blade-coating-w4600-app-guide-and-technical.data.pdf, 2014, 3m wind blade protection coating w4600 technical data sheet and application guide.
[61] G. ASTM, G 73–98, Standard Practice for Liquid Impingement Erosion Testing, Annual Book of ASTM Standards vol. 3.
[62] S. Dong, C.-S. Jiao, S.-S. Tao, Joint return probability analysis of wind speed and rainfall intensity in typhoon-affected sea area, Nat. Hazards 86 (3) (2017) 1193–1205.

Abbreviation

FEM: Finite Element Method
LEE: Leading Edge Erosion
LE: Leading Edge
CFD: Computational Fluid Dynamics
WTB: Wind Turbine Blade
FSI: Fluid Structure Interaction
OWT: Offshore Wind Turbine
MW: Megawatt
MLE: Maximum Likelihood Estimation
RPM: Rotation Per Minute
3M: Minnesota Mining and Manufacturing company
PDF: Probability Density Function
CDF: Cumulative Distribution Function
ASTM: American Society for Testing and Materials
DSD: Droplet Size Distribution
KNMI: Koninklijk Nederlands Meterorologisch Instituut
WARER: Whirling Arm Rain Erosion Rig
SPIFT: Single Point Impact Fatigue Tester
DTU: Danmarks Tekniske Universitet
TNO: Toegepast Natuurwetenschappelijk Onderzoek
NREL: National Renewable Energy Laboratory
USA: United States of America
EU: European Union

Nomenclature

ρ_s: Material density (kg/m^3)
c_s: Speed of sound in the coating material (m/s)
ρ_w: Density of water (kg/m^3)
c_w: Speed of sound in water (m/s)

V_{tg}: Terminal velocity of rain drop (m/s)
φ_d: Droplet diameter (mm)
I: Rainfall intensity (mm/hr)
U_w: Mean wind speed at hub height (m/s)
$f_I(I)$: Marginal distribution of rainfall intensity
$f_{\varphi_d|I}(\varphi_d|I)$: PDF: Droplet size distribution (DSD)
$F_{\varphi_d|I}(\varphi_d|I)$: CDF: Droplet size distribution (DSD)
$f_{I,\varphi_d}(I,\varphi_d)$: Joint probability density function of I and φ_d
$P(I)$: Percentage of rain duration for different intensities ($\% \cdot 0.01$)
$f_{U_w}(U_w)$: Marginal distribution of mean wind speed at hub height
D_{50}: Median droplet size (mm)
λ: Parameter of exponential distribution
$\dot{D}_i^{ST}(I,\varphi_d,U_w)$: Short term erosion damage rate (hr^{-1})
$\dot{D}_i^{LT}(I,\varphi_d,U_w)$: Probabilistic erosion damage rate (hr^{-1})
$\dot{D}_i^{LT}$: Long-term erosion damage rate (hr^{-1})
a: Scale parameter of Weibull distribution
n: Shape parameter of Weibull distribution
A, p, N, q: Constants of DSD
q: Number of droplets per unit volume of rainfall
V_{blade}: Blade tip speed (m/s)
V_{imp}: Impact velocity (m/s)
ν: Poisson's ratio
N_{ic}: Number of impacts during the incubation period
$\dot{N}$: Number of impacts at the blade tip
E: Young's modulus of material -(MPa)
σ_u: Tensile ultimate strength of coating material -(MPa)
m: Wohler's slope
t_{years}: Expected lifetime of the blade coating system (yr)
$\hat{\beta}_d$: Droplet impingement efficiency
μ: Mean: distribution parameter of lognormal distribution
σ: Standard deviation: distribution parameter of lognormal distribution
H_o: Null Hypothesis
α_s: Significance level used in hypothesis test
z_r: Reference wind turbine height (10m)
z: Hub height
α: Shape parameter of gamma distribution
β: Scale parameter of gamma distribution
i: Cases of rain intensity occurring at the wind turbine site
j: Cases of droplet size occurring at the wind turbine site
k: Cases of mean wind speed occurring at the wind turbine site and at hub height
χ^2: chi-square statistic
χ^2_{cric}: chi-square critical
O_k: Observed counts
E_k: Expected counts